Delft University of Technology

Extended CSDT model for shear capacity assessments of bridge deck slabs

de Sousa, Alex M.D. ; Lantsoght, Eva O.L.; Yang, Yuguang ; El Debs, Mounir K.

DOI
10.1016/j.engstruct.2021.111897

Publication date
2021

Document Version
Accepted author manuscript

Published in
Engineering Structures

Citation (APA)
de Sousa, A. M. D., Lantsoght, E. O. L., Yang, Y., & El Debs, M. K. (2021). Extended CSDT model for shear capacity assessments of bridge deck slabs. *Engineering Structures*, *234*, 1-16. Article 111897. https://doi.org/10.1016/j.engstruct.2021.111897

Important note
To cite this publication, please use the final published version (if applicable).
Please check the document version above.

Copyright
Other than for strictly personal use, it is not permitted to download, forward or distribute the text or part of it, without the consent of the author(s) and/or copyright holder(s), unless the work is under an open content license such as Creative Commons.

Takedown policy
Please contact us and provide details if you believe this document breaches copyrights.
We will remove access to the work immediately and investigate your claim.

This work is downloaded from Delft University of Technology.
For technical reasons the number of authors shown on this cover page is limited to a maximum of 10.

© 2021 Manuscript version made available under CC-BY-NC-ND 4.0 license https://creativecommons.org/licenses/by-nc-nd/4.0/

Title: Extended CSDT model for shear capacity assessments of bridge deck slabs

Running head: Shear capacity of bridge deck slabs with the CSDT model

NOTE: This is the peer-reviewed version of the following article: de Sousa AMD, Lantsoght EOL, Yang Y, El Debs MK. Extended CSDT model for shear capacity assessments of bridge deck slabs. Eng Struct 2021;234:111897, which has been published in final form at [https://doi.org/10.1016/j.engstruct.2021.111897]. This article may be used for non-commercial purposes in accordance with Elsevier Terms and Conditions for Use of Self-Archived Versions.

Author 1
P.h.D. candidate Alex M. D. de Sousa
University of São Paulo, São Carlos School of Engineering
Department of Structural Engineering
Av. Trabalhador Sãocarlense, 400, 13566-590,
Sao Carlos, Brazil
Phone: (+55) 16 3373 9474
Orcid ID: 0000-0003-0424-4080
alex_dantas@usp.br

Author 2
Dr. ir. Eva O.L. Lantsoght
Politécnico, Universidad San Francisco de Quito
Diego de Robles y Pampite, Cumbaya, Quito, Ecuador
Phone: (+593) 2 297-1700
Orcid ID: 0000-0003-4548-7644
elantsoght@usfq.edu.ec
Concrete Structures, Delft University of Technology
P.O. Box 5048, 2600 GA Delft, The Netherlands
E.O.L.Lantsoght@tudelft.nl

Author 3
Dr. ir. Yuguang Yang
Concrete Structures, Delft University of Technology,
P.O. Box 5048, 2600 GA Delft, The Netherlands
yuguang.yang@tudelft.nl

Author 4
Dr. ir. Mounir K. El Debs
University of São Paulo, São Carlos School of Engineering,
Department of Structural Engineering,
Av. Trabalhador Sãocarlense, 400, 13566-590,
São Carlos, Brazil
Phone: (+55) 16 3373 9474
Orcid ID: 0000-0001-5955-7936
mkdebs@sc.usp.br

Abstract

The shear strength evaluation of reinforced concrete bridge deck slabs by accurate models can indicate strength reserves and avoid costly operations necessary for the extension of their lifetime. This article introduces an approach that extends the Critical Shear Displacement Theory model (CSDT) for reaching higher levels of approximation of the shear strength for slabs subjected to concentrated loads close to the support. A database with 141 tests of wide reinforced concrete members under concentrated loads close to the support failing in one-way shear was built. The tests represented typical loads in bridge slabs and were assessed through a combination of CSDT with different models of effective shear width. In other analyses, the entire database with 214 test results of slabs failing by different mechanisms was evaluated and a general effective shear width model was proposed (GESW). The best results, which are a function of the effective shear width model used, reached a mean ratio between experimental and predicted shear capacities of 1.06 with a coefficient of variation of 14%, which is similar to that reported by some studies including linear and non-linear finite element analyses. Furthermore, this level of accuracy was insensitive to the shear slenderness and support conditions of the tests. The extended CSDT predicted the shear capacity of bridge deck slabs in preliminary analyses more precise than semi-empirical models provided in the current design codes, and the level of accuracy is comparable to methods using Linear Finite Element Analyses (LFEA). Moreover, our proposed combination of the CSDT with a general effective shear width model (GESW) provides reasonable levels of accuracy for slabs under concentrated loads regardless of the failure mode of the tests. Therefore, the proposed approaches can be applied to bridge deck slabs, which are subjected to a variety of loading and support conditions.

Keywords: Bridge deck slabs; Critical shear displacement theory; Database; Effective shear width; Reinforced concrete; Shear strength;

1 INTRODUCTION

The shear capacity of bridge deck slabs attracted attention from several researchers and bridge owners in Europe in the last decade since a large number of these structures built between 1960 and 1980 have reached the end of their originally devised service life [1–4]. A number of these bridges do not rate sufficiently for shear according to the currently governing codes, despite no signal of distress. This result indicated that widely accepted semi-empirical approaches of design could be overly conservative. Since conservative predictions of shear strength could indicate the need for replacement or retrofitting of these structures, the identification of more accurate approaches for predicting the shear capacity of bridge deck slabs involves an economic and environmental issue, beyond the user's safety. Apart from that, the design of wide reinforced concrete members prioritizes solutions without shear reinforcement, since installing shear reinforcement is not cost-effective and may result in reinforcement congestion. Therefore, also in design, the use of precise one-way shear models can be essential to ensure adequate safety levels for members without stirrups.

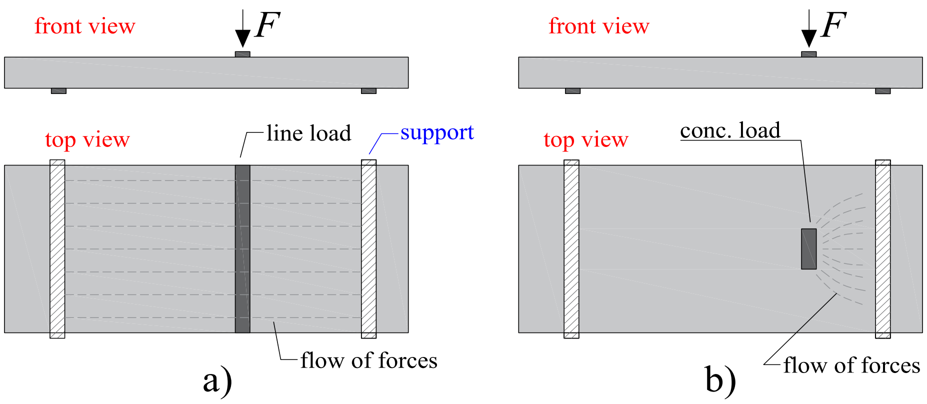

Figure 1 - Slabs loaded (a) over the entire width analyses by de Sousa et al. [5] and b) under concentrated loads in non-symmetrical conditions subjected to one-way shear failures.

In a previous study on wide beams and one-way slabs loaded over the entire width [5] (Figure 1a), it was identified that the Critical Shear Displacement Theory model (CSDT [6,7]) showed the best levels of accuracy and precision compared to many semi-empirical and mechanical models of shear strength, with the mean ratio between experimental and predicted shear capacities of 1.15 and COV of 16%. Different from previous publications [8,9], de Sousa et al. [5] applied the analyses for both slender and non-slender members, in addition to different support and loading conditions. Therefore, it was decided to further assess the CSDT model for slabs under concentrated loads in non-symmetrical conditions (Figure 1b), with emphasis on the one-way shear capacity.

Although the number of studies on shear in reinforced concrete members increased significantly in the last decade, most of them were focused on the level of precision by semi-empirical code models of shear strength [3,10–13]. In publications that include mechanical-based models [2,14–16], the analyses focused on one kind of support conditions and hence, covered a reduced number of tests. At the same time, only a limited number of studies addressed the fact the slabs under concentrated loads may show a transitional failure mode between one-way and two-way shear [17]. As a consequence, if the governing failure mode is unknown, the use of a one-way shear model to assess members whose governing failure mode is punching shear may lead to unsafe predictions of shear strength. Therefore, we identified the need for a more comprehensive study, covering slabs under different support conditions, assessed by a mechanical-based model such as the CSDT and accounting for different failure modes that may take place.

In this study, the application of the Critical Shear Displacement Theory Model (CSDT) [6,7] is extended to the assessment of one-way shear capacity of wide reinforced concrete members under concentrated loads in non-symmetrical conditions (Figure 1b). Different from previous studies, we covered a variety of support conditions (cantilevers, simply supported and continuous members; members under different loading conditions such as single loads and double loads close to the support; and we provided recommendations when the governing failure mode is known or unknown.

The literature was reviewed in order to discuss the influence of the shear slenderness over the governing failure mode of slabs. Furthermore, models to account the slab behavior under concentrated loads and approaches to account improved shear capacities for loads close to the support are described and assessed in the paper. Different databases were used to derive and validate each recommendation for cases where the governing failure mode is known or unknown and how to account for the higher shear strength for slabs under concentrated loads close to the support. The application limits and benefits of each recommendation are highlighted in the paper, which also compares the results with well-established models from the literature.

2 LITERATURE REVIEW

2.1 Shear failure modes

One-way shear failure and two-way shear failure or punching can be critical in bridge deck slabs without shear reinforcement [2,17]. The critical failure mode can vary according to the gradient of shear forces close to concentrated loads [18]. For slabs loaded over the entire width, the shear force per unit length is almost constant over the shear span if the self-weight is neglected. On the other hand, for flat slabs under concentric loads, the gradient of unitary shear forces (shear force per unit length of the critical perimeter) becomes higher near the loaded region, since the perimeter of the shear transfer is reduced [18]. Some studies suggest the combination of shear field analyses with one-way and two-way shear models for the determination of the critical failure mode [2,19], whereas others already highlight that some tests can show the same capacity for one-way and two-way shear [20]. This means that the ratio between the one-way shear effects (V_{exp}) from the acting punching load (P_{exp}) with the calculated one-way shear capacity (V_{calc}) is very similar to the ratio between the acting punching load (P_{exp}) with the calculated punching capacity (P_{calc}). Since the most critical failure mode may change according to the geometry of the load, slab, and support conditions [14], the check of both failure modes is essential for the assessment of existing structures, where a precise estimation of the shear capacity is required [20].

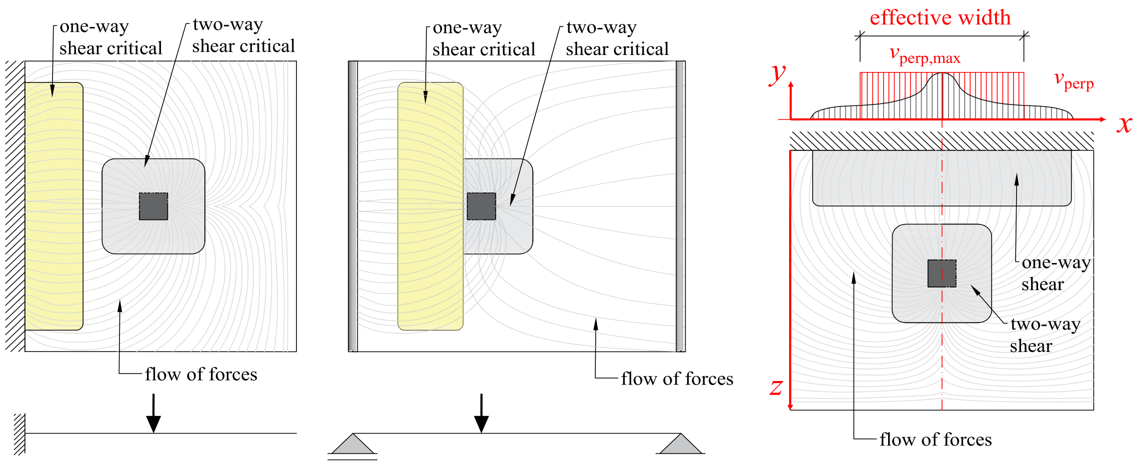

a) b) c)

Figure 2 - Critical regions of one-way and two-way shear for a) cantilever (adapted from Reiβen [21] and b) simply supported members; c) effective width definition for one-way shear analyses (adapted from Reiβen [21])

Figure 2 shows the complex transition between these two failure modes. For cantilever slabs under concentrated loads, for instance, regions of critical one-way and two-way shear can be better differentiated for large shear spans (Figure 2a), whereas for simply supported slabs, such regions intercept each other (Figure 2b). Different studies have agreed on the existence of a trend for the punching failure mode to become critical for higher shear slenderness [17,20–23].

Attention should be drawn to the fact that both one-way shear expressions and punching shear expressions were derived and calibrated using lab tests designed with idealized boundary conditions. For instance, one-way shear expressions were derived based on simply supported beam tests with point loads [24]; and punching shear expressions were based on punching tests on idealized slab-column connections. One-way slabs typically have boundary conditions and failure modes between the two types of failure modes, therefore, none of these two types of expressions were developed for such structures.

2.2 Effective shear width

When slabs are subjected to concentrated loads, an effective shear width needs to be defined together with a one-way shear model, since not the full slab width carries the same shear stress [2,25]. Figure 2c shows the profile of shear stresses over the support as well as the distribution of shear stresses around the load [2,3,22,25]. Integrating the shear stress v_{perp} over the width results in the sectional shear at failure. However, for design, deriving the shear stress distribution over the support is not practical, and therefore a uniform shear stress is commonly considered over a reduced width, which is the effective shear width (Figure 2c). The integral of the maximum shear stress $v_{perp,max}$ over the effective width should theoretically approach the integral of the shear stress v_{perp} over the full width. The values of $v_{perp,max}$ can be determined by linear elastic finite element (LEFE) analysis with shell elements adjusting the shear modulus G and the Poisson ratio v to account for cracking and load redistribution [2,11,19,26,27]. However, the relevant section may vary according to the shear model (between d and $d/2$ away from discontinuities or at the support) and according to the support and loading conditions [20].

In practice, the effective width is usually defined based on a method of horizontal load spreading from the concentrated load to the support or a section parallel to the support (Figure 3). However, some publications already highlighted that the French method (as shown in Figure 3) could overestimate the effective width in more than 30% for tests with shear slenderness higher than 5 [28]. Physically, this horizontal load spreading can be influenced by factors such as the reinforcement ratio in the transverse direction [1,3], available member width [3,29], and size of the concentrated load [21].

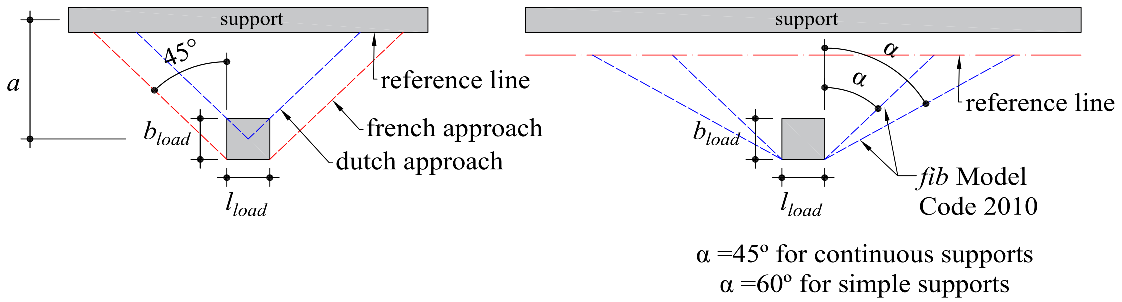

Figure 3 – Models of effective shear width used in design guides with respective reference lines.

Table 1 shows an overview of expressions for the effective width in the one-way shear strength of reinforced concrete members under concentrated loads at the slab mid-width. For loads close to the edge, however, the effective shear width are equal to $b_r + b_{eff}/2$, where b_r is the distance from the load axe to the free edge of one-way slabs. Table 1 displays some replaced design code models, e.g. the Brazilian code from 1980 [30], since the current codes do not provide recommendations related to the effective shear width. According to the table, most code provisions [30–34] and some proposed in the literature [22,35,36] assume the effective width increases for larger shear spans. This idea relies on the yield line theory [37] and experimental investigations [38], which account for shear forces spreading on elastic plates under concentrated loads, also confirmed partially by LEFE analyses [2]. In summary, most available models of effective shear width do not take into account the change in the governing failure mode according to the position of the load [32,34] or were calibrated for specific supporting conditions [15]. More consistent models of effective shear width, on the other hand, usually require LEFE analyses [2].

Table 1 - Overview of analytical models that predict the effective width in analyses of one-way shear strength of wide RC members under concentrated loads close to the support.

Old Dutch approach [31] (replaced)	$$b_{eff\,1} = b_{load} + 2 \cdot a_v \quad (1)$$
French [32]	$$b_{eff\,2} = l_{load} + 2 \cdot (b_{load} + a_v) \quad (2)$$
Brazilian code [30] (replaced)	$$b_0 = b_{load} + h \quad (3)$$ For cantilever members: $$b_{NBR} = b_0 + 0.5 \cdot a \cdot \left(1 - \frac{b_0}{\ell}\right) \leq \max\left(b_{slab}; a + 0.5 \cdot b_{NBR}\right) \quad (4)$$ For other static systems: $$b_{NBR} = b_0 + a \cdot \left(1 - \frac{b_0}{l}\right) \leq \max\left(b_{slab}; a + 0.5 \cdot b_{NBR}\right) \quad (5)$$
German guideline [39] (replaced)	$$t = b_{load} + 2 \cdot h_1 + h \quad (6)$$ For cantilever members:

	$b_{H240} = \begin{cases} 0.2\ell_k + 0.3a & \text{for: } 0.2\ell_k < a < \ell_k;\ t_y < 0.2\ell_k;\ t_x < 0,2\ell_k \\ t_y + 0.3a & \text{for: } 0.2\ell_k < a < \ell_k;\ 0.2\ell_k < t_y < 0.4\ell_k;\ t_x < 0.2\ell_k \end{cases}$ (7) For simply supported members: $b_{H240} = t_y + 0.5a \quad \text{for: } 0 < a < \ell,\ t_y \le 0.8\ell,\ t_x \le \ell$ (8) For loads close to simple support of continuous members: $b_{H240} = t_y + 0.4a \quad \text{for: } 0.2\ell < a < \ell,\ t_y \le 0.4\cdot\ell,\ t_x \le 0.2\ell$ (9) For loads close to continuous supports $b_{H240} = t_y + 0.3a \quad \text{for: } 0.2\ell < a < \ell,\ t_y \le 0.4\ell,\ t_x \le 0.2\ell$ (10)
Swedish Code [40] (replaced)	$b_{BBK} = \max \begin{cases} b_{load} + 7\cdot d_l \\ 0.65\cdot\left(b_{load} + l_{load}\right) + 10.65\cdot d_l \end{cases}$ (11)
fib Model Code 2010 [34]	$b_{effMC} = l_{load} + 2\cdot\left(b_{load} + a_v - \min\left(d_l; a_v/2\right)\right)\cdot\tan\theta$ (12) $\theta = \begin{cases} 45^{\circ}, \text{ cantilever of continuous members} \\ 60^{\circ}, \text{ if load is close to simple support} \end{cases}$
Zheng et al. [41]	$b_{Zh} = l_{load} + l_{span}\cdot\left(1 - r_{cp}\right)\cdot\tan\Phi$ (13) $r_{cp} = \frac{b_{load}}{l_{span}} \le 0.4$ (14) $\Phi\left(^{\circ}\right) = 23.3\cdot r_{cp} + 35.1$ (15)
Bauer [35]	$b_{eff,Bauer} = l_{load} + b_{eff1}$ (16)
Vidaković and Halvonik [36]	For cantilever members: $b_{eff,VH} = l_{load} + 2\cdot\left(b_{load} + \min\left(2\cdot d_l; a_v\right)\right)$ (17)
Reiβen and Hegger [42,43]	For simply supported members: $b_{eff} = b\cdot\lambda_b\cdot\lambda_{\rho q}\cdot\lambda_l\cdot\lambda_{a/d}$ (18) $\lambda_b = 1.2 - 0.12\cdot b \le 1, \text{ for } b \le 5.5\ m$ $\lambda_{\rho q} = 0.74 + 2.2\cdot\rho_q^{0.4}, \text{ for } 0 \le \rho_q \le 0.7\%$ $\lambda_l = 0.81 + 0.045\cdot l \le 1.04, \text{ for } l \ge 2\ m$ $\lambda_{a/d} = 1.8 - 0.19\cdot a/d, \text{ for } 2.91 \le a/d \le 5.41$ (19)
Reiβen [21]	$b_{\text{Reiβen}} = 7\cdot d_{l,load} + k_{bf}\cdot l_{load}$ (20) With: $d_{l,load} \le 0.40$ m $k_{bf} = -\frac{5}{8}\cdot\max\left(a_1; a_2\right)/d + \frac{9}{4}, \begin{cases} \le 1 \\ \ge 0.5 \end{cases}$ (21)
Rombach and Velasco [44]	For LEFE analyses: $b_{RV} = 0.6 + 0.95\cdot h + 1.15\cdot a$ (22)
Natário et al. [2]	For LEFE analyses on cantilever slabs: $b_{eff} = F_{aplied}/v_{avg,4d}$ (23)
Shu et al. [45]	For NLFE analyses on cantilever slabs:

	$$b_{eff,Shu} = b_w \cdot \beta_{w1} = b_w \cdot \frac{v_{E,avg}}{v_{R,code}} \qquad (24)$$

2.3 Failure modes and shear transfer mechanisms in one-way shear

Since Kani [46] and Leonhardt and Walther [47], it has been known that different shear failure modes can occur as a function of the shear slenderness *M/Vd* and that shear strength increases considerably for short members. Figure 4 shows the way the nominal shear strength of wide reinforced concrete members (width-to-effective depth b/d>1) increases as the shear slenderness decreases for tests under concentrated loads (CL) [5]. The figure also shows how the critical shear crack shape changes according to the shear slenderness [48]. For concentrated loads close to the support, or shear slenderness M/Vd < 2.5, direct load transfer may occur by compressive struts improving the shear capacity. Such members are usually called non-slender members or deep beams for beam-shaped members. The higher concentration of compressive stresses between load and support usually leads to the crushing of concrete at failure [49]. This failure mode is called shear-compression failure [7].

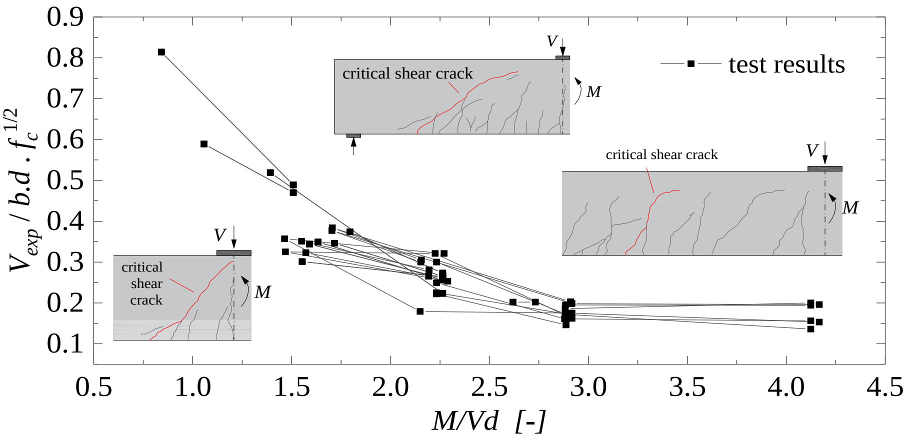

Figure 4 - Shear slenderness effect on the one-way shear behavior of wide reinforced concrete members without stirrups. Adapted from de Sousa et al. [5].

Commonly, the same shear strength model derived for flexure-shear failures is used for the design and verification of shear strength of non-slender members through the application of a factor that reduces the acting shear force V_{Ed} or improves the shear capacity V_R in a critical section, as suggested in NEN 1992-1-1:2005 [50] and *fib* Model Code 2010 [34]. The shear reduction factor β from NEN-EN 1992-1-1:2005 [50] first considered only the bending moment effect on the compression chord or cantilever action [51]. This means that only the effect of lower crack openings and large compression chord depth were taken into account. In fact, the shear strength enhancement for non-slender members is caused by a combination of the following mechanisms: (i) higher compression chord capacity (cantilever action [18,51]) due to the large compression zone depth [49] and (ii) direct load transfer that occurs by compression arch beyond the inclined cracking load (or strut if it has a straight shape), also named arching action [17,52]. In the literature, both mechanisms are cited as the source of improved arching action [2].

Table 2 shows a summary of the main expressions suggested by different references to account for the increase in shear capacity for loads close to supports – past codes used the shear span to depth ratio *a/d* as the main parameter. The model proposed by Reiβen [21] was calibrated for the European code shear model and took into account the ratio $max\{a_1;a_2\}/d$ (a_1 and a_2 refer to the distances from the section of zero bending moment to the support and load axes, respectively) in such a way that it provides precise estimations of strength for both simply supported and continuous members. In this text, the ratio $max\{a_1;a_2\}/d$ has the same meaning as the shear slenderness M/Vd. Since the influence of the shear slenderness is already taken into account in the shear models from *fib* Model Code 2010 and SIA 262:2013 by the calculations of the internal forces, the β factor takes into account the improved arching action only by the clear shear span-to-effective depth ratio a_v/d as a more conservative approach.

Table 2 - Expressions for reducing the acting shear load V_E for non-slender members according to different references.

Reference	Model
ABNT NBR 6118:2014 [53] – Brazilian code DIN 1045:1988 [54] – German code	$\beta = \frac{a}{2 \cdot d}$ (25)
DIN 1045-1:2001 [55]– German code	$\beta = \frac{x}{2 \cdot d}$ (26) x measured from load axis to support edge
NEN-EN 1992-1-1:2005 [50] – European code	$\beta_{EC} = \frac{a_v}{2 \cdot d} \begin{cases} \leq 1.00 \\ \geq 0.25 \end{cases}$ (27)
fib Model Code 2010 [34]	$\beta_{MC} = \frac{a_v}{2 \cdot d} \begin{cases} \leq 1.00 \\ \geq 0.50 \end{cases}$ (28)
SIA 262:2013 [56] – Swiss code	$\beta_{SIA} = \frac{a_v}{2 \cdot d}$ (29)
Reiβen [21]	$\beta_{\mathrm{R16}} = \frac{\max\{a_1;a_2\}}{2.8 \cdot d} \begin{cases} \leq 1.0 \\ \geq 0.4 \end{cases}$ (30)
Natário et al. [2]	$\beta_{\mathrm{Nat14}} = \frac{a_v}{2.75 \cdot d} \begin{cases} \leq 1.00 \\ \geq 0.50 \end{cases}$ (31)
Yang et al. [57]	$\beta[M/Vd] = \frac{M}{Vd \cdot 2} \leq 1$ (32)

2.4 Critical Shear Displacement Theory Model

The Critical Shear Displacement Theory (CSDT) [6,7] assumes that a critical inclined crack starts from a major flexural crack, which will lead to collapse when the shear displacement Δ of the crack reaches a critical value and causes a secondary crack (dowel crack) along the reinforcement. A dowel crack causes the detachment of the tensile reinforcement from the concrete along the shear span, which significantly reduces the lateral confinement on the crack and the member flexural stiffness [7]. Due to the opening of the main crack, an additional vertical shear displacement is required for the recovery of the previous shear stress level in the crack, which feeds the growth of flexure-shear cracks and leads to a brittle collapse of the member [7].

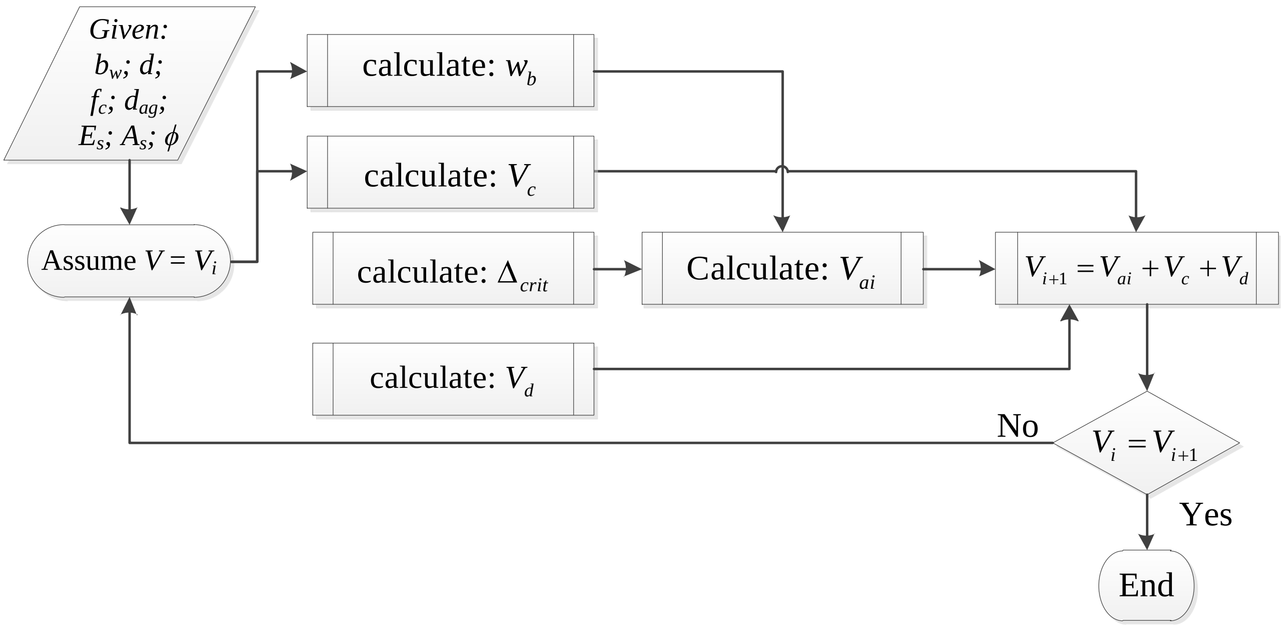

Figure 5 - Flowchart of the calculations using the CSDT model

The CSDT assumes that the shear capacity of RC members without stirrups is resisted by (i) compression chord capacity [58], (ii) dowel action [59], and (iii) aggregate interlock [60]. The contribution of the residual tensile strength of concrete is neglected at failure [7], and the aggregate interlock contribution is a function of the crack width w_b at the level of the tensile reinforcement and derived from the shear displacement Δ [61]. Figure 5 and Table 3 show, respectively, a flowchart of the calculations for the prediction of shear capacity and the base equations used.

Table 3 – Expressions used in the CSDT [6]

Model	**Expression**
General [6]	$V_u = V_c + V_{ai} + V_d$ (33)
Compression chord [58]	$V_c = \frac{2}{3}\frac{z_c}{z}V = \frac{d - s_{cr}}{d + s_{cr}}V$ (34)
Aggregate interlock [6]	$V_{ai} = \text{either of } \begin{cases} R_{ai}\sigma_{pu}\int_0^{s_{cr}} b\left(A_x(\Delta, w) - \mu A_y(\Delta, w)\right)ds \\ R_{ai} f_c^{0.56} s_{cr} b \frac{0.03}{w_b - 0.01}\left(-978\Delta^2 + 85\Delta - 0.27\right) \\ R_{ai}\int_0^{s_{cr}} \tau_{ai}(\Delta, w) b ds \end{cases}$ (35)
Dowel action [59]	$V_d = 1.64 b_n \phi \sqrt[3]{f_c}$, f_c in [MPa] (36)
Factors	**Expression**
Height of fully developed crack	$s_{cr} = \left(1 + \rho_l n_e - \sqrt{2\rho_l n_e + \left(\rho_l n_e\right)^2}\right)d$ (37)
Critical shear displacement	$\Delta_{cr} = \frac{25d}{30610\phi} + 0.0022 \le 0.025$ mm (38)
Crack width at the bottom of the crack	$w_b = \frac{M}{zA_s E_s} l_{cr,m}$ (39)
Reduction factor for aggregate interlock for high-strength concrete [6]	$R_{ai} = 0.85 \cdot \sqrt{\left(\frac{7.2}{f_c - 40} + 1\right)^2 - 1} + 0.34$ with f_c in MPa and f_c > 65 MPa (40)

3 DATABASES

This study assumes that checking both shear-critical failure modes, one-way and two-way shear, is essential to identify the governing failure modes of existing bridge deck slabs. Therefore, a careful classification of the failure modes of tests from the literature is of paramount importance to understand the limits of application of the available one-way and two-way shear models. Moreover, this classification allows a fairer assessment of the precision of one-way and two-way shear models, as well as models of effective shear width for slabs under concentrated loads.

This study will discuss the results of three database subsets which are published in the public domain [62]: (i) wide beams and one-way slabs loaded over the entire width failing in one-way shear (Database A); (ii) slabs under a single concentrated load failing in one-way shear, two-way shear or a combination of both (Database B0) and; (iii) slabs subjected to double loads close to the line support (Database C).

3.1 Database filtering and organization

The Database B0 includes 214 test results of slabs under single concentrated loads that were classified according to the main failure mode in (i) wide beam shear or one-way shear (WB), (ii) punching shear (P) and (iii) transition mode between wide beam shear and punching shear (WB/P). Since this study focuses on the one-way shear model, tests with signs of punching failure were initially removed from the database B0, which resulted in the database B1 (141 tests). This filtering was based on (i) the cracking pattern of the members, when available in the original references and (ii) the classification reported by other authors [10,63], which was also based on the cracking pattern and (iii) in the classification of Natário [20], who combined shear fields from LEFE analyses with one-way shear and punching shear models according to the Critical Shear Crack Theory (CSCT) [2,19,20]. The main criteria used for the removal of members because of a punching failure in this study were (i) absence of a critical shear crack visible on the edge of the members and (ii) position at which the critical shear crack intercepted the middle depth of the member when the cut view was available. When the internal cracking pattern was not shown in the references, it was considered a punching failure if the cracking pattern was predominantly formed by radial and tangential cracks or if a conical crack could be seen.

The database B1 of slabs under concentrated loads after removing punching tests comprehends 141 test results from the following references: Cullington et al. [64], Lantsoght [63], Reiβen [21], Lubell [65], Bui et al. [66], Regan [67], Regan and Rezai-Jarobi [68], Vaz Rodriguez et al. [69], Rombach and Latte [70,71], Natário et al. [2,72], Rombach and Henze [73], and Vida et al. [74]. The database entries include the effect of self-weight on the calculated shear capacities and on the shear slenderness parameters for continuous members.

The database B1, whose organization was inspired by those of Lantsoght et al. [10], Reiβen [21] and Henze et al. [11], has been published in the public domain [62] and includes 46 tests on cantilever members (CT), 33 tests with concentrated loads close to the internal support of continuous members (CS), and 62 tests with concentrated loads close to the simple supports (SS). It also includes two modes of one-way shear failures, namely shear-compression failures for non-slender members, or shear slenderness $M/Vd < 2.5$ (55 tests ≡ 39 %), and flexure-shear failures for slender members, or shear slenderness $M/Vd \geq 2.5$ (86 tests ≡ 61%).

Figure 6 displays the main geometrical loading parameters in the database for members with continuity over line supports and subjected to a combination of concentrated loads and line loads. The same definitions have been used for other structural systems.

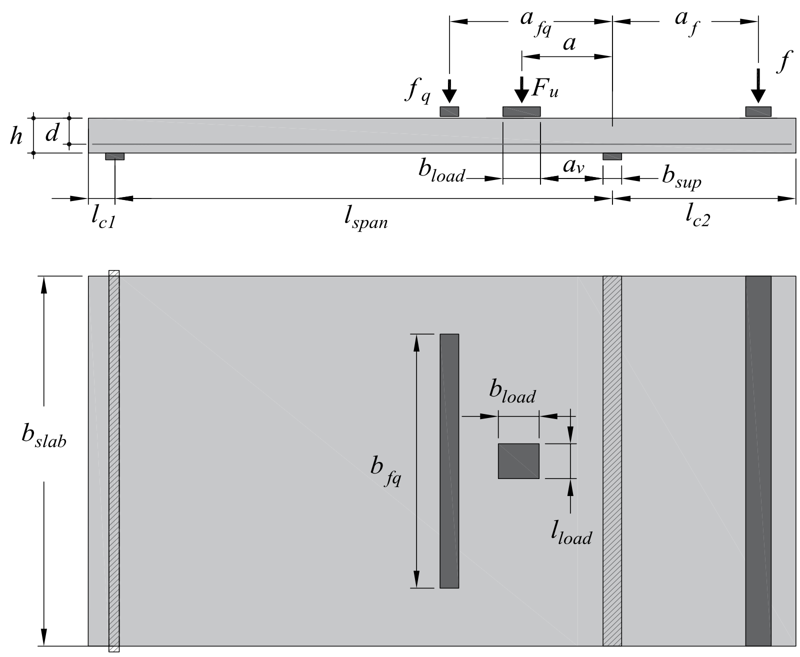

Figure 6 - Geometrical parameters of wide members with continuity over the support.

Figure 7 shows the distributions of the parameters related to the tests included in the database B1. Similar to beam-databases [75,76], most experiments were performed for members of thicknesses less than 600 mm (Figure 7a) and on wide members whose ratio between the slab width and load dimensions in the width direction was higher than 5 (Figure 7b). The full width of members with $b_{slab}/l_{load} < 5$ was probably activated in the test, depending on the distance from the load to the support. However, as some models of effective width are overly conservative, some predictions may indicate that the full width was not mobilized. Figure 7c shows that the b_{slab}/h aspect ratio (Figure 11c) was higher than 5 in more than 75% of the tests, and Figure 7d highlights the number of tests in the database performed with a shear slenderness M/Vd between 2 and 3. This range indicates that a considerable number of tests were subjected to a transitional failure mode between shear-compression and flexure-shear. Figure 7e show that 16 tests from the database have a concrete compressive strength larger than 60 MPa and, hence, the level of accuracy for members with reduced aggregate interlock may be assessed. Figure 7f shows that the longitudinal reinforcement ratio ranges between 0.6 and 1.8%, where the larger ratios may not be representative of those used in bridge deck slabs.

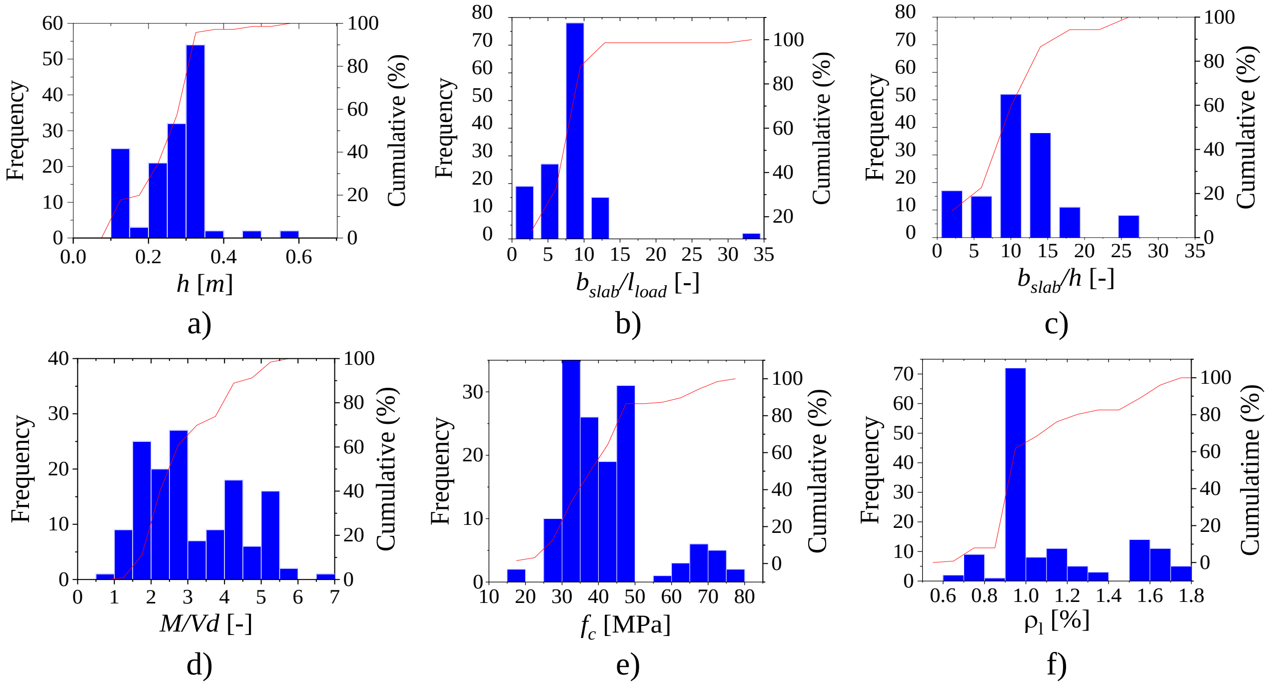

Figure 7 – Distribution of parameters in the database B1 for the following parameters: a) thickness of the slab at the support edge, b) ratio of slab width-to-load dimension in the width direction, c) ratio of slab width-to-effective depth, d) shear slenderness; e) concrete compressive strength and f) longitudinal reinforcement ratio.

4 PROPOSED RECOMMENDATIONS

4.1 Section for internal forces calculations

Since most mechanical based models of shear strength were derived for shear slenderness M/Vd higher than 2.5, the assumption of the section far from d or $d/2$ from the highest bending moment axes [6,77] or from geometrical discontinuity [34] does not play an important influence. However, when using these models for lower slenderness (M/Vd < 2.5), the location of this section assumes a major influence. Because of this, a previous investigation was made in order to identify the section that could balance precision and safety for the ratio V_{exp}/V_{cal} in both ranges of shear slenderness and for different support conditions (Figure 8b,c,d). Assuming that the shear capacity is reduced due to an increase in the opening of the critical shear crack [6,77,78], the control section for the calculations of the internal forces M_{Ed} and V_{Ed} remain at sections close to the higher bending moment for all models. However, the critical section at the support edge of cantilever slabs was used instead of the section at d or $d/2$ from the support edge in order to reach better predictions for these support conditions [5].

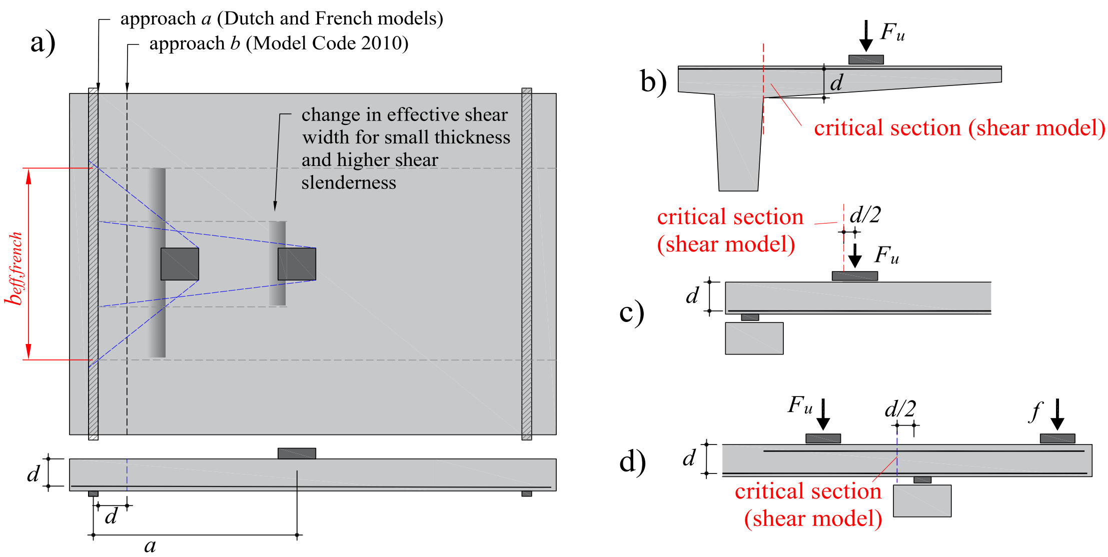

Figure 8 – a) reference lines to calculate the effective shear width in French model [32] and proposed approach; critical sections used for b) cantilever members, c) simply supported members, and d) continuous members.

4.2 Arching action

This study proposes to combine the CSDT result with a semi-empirical coefficient β based on the ratio a_v/d (Equation (41)) to extend the CSDT model to predict the shear capacity of non-slender members without additional iterative calculations:

$$\beta_{\mathrm{Prop}} = \frac{a_v}{2.5 \cdot d} \begin{cases} \leq 1.00 \\ \geq 0.40 \end{cases} \tag{41}$$

The combination of the CSDT with reduction factor β for non-slender members should be understood as an engineering approach comparable to empirical simplifications used by most design codes [34,50] and strain-based models [2]. Theoretically, this approach is not exact because the shear failure mechanism for non-slender members is different from that for slender ones: the shape and relative contribution of the main shear-transfer mechanisms vary significantly when the shear slenderness decreases since the vertical branch of the assumed crack profile of the critical shear crack becomes not representative anymore (Figure 9b).

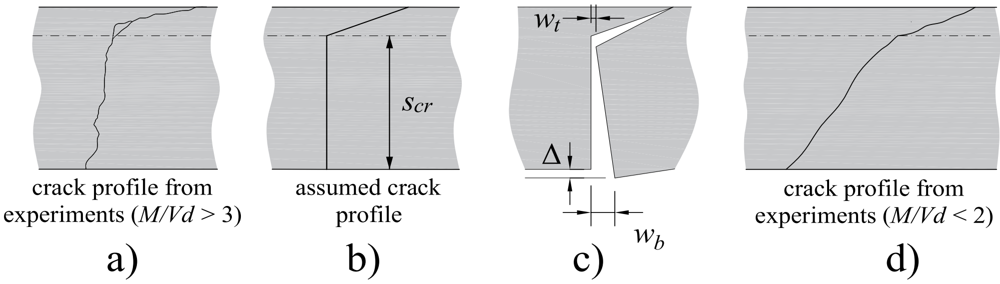

Figure 9 - a) and b) Crack profile simplification for specimens with *M/Vd* > 3, c) main parameters of CSDT, and d) crack profile for non-slender members (*M/Vd* < 2).

For lower shear slenderness, the inclination of the major flexural crack increases in such a way that the contribution of the aggregate interlock decreases significantly, while the contribution of the compression chord V_c increases according to internal equilibrium [79]. The use of strut-and-tie models for continuous members with maximum shear slenderness *M/Vd* < 2 may better represent the problem [80]: plane sections do not remain plane, and shear strains become dominant for those members [81]. However, this approach may not be practical for the slabs studied since the problem is strongly three-dimensional. As such, for practical purposes, we consider the choice of including β as adequate.

4.3 Effective shear width

In design and assessment of existing structures, two kinds of analyses may occur (i) the governing failure mode is unknown, and a conservative prediction of the shear capacity may be adequate for preliminary design, and (ii) a more precise estimation of the shear capacity is required, usually in the assessment of existing structures preliminarily rated as critical in shear [82]. In the latter case, a detailed analysis of the governing failure mode would be essential to determine the shear capacity, which requires LEFE analyses combined with a mechanical-based model, such as conducted by Natário [20] or using one-way and two-way shear models adjusted to slabs under concentrated loads in non-symmetrical conditions.

Since the governing failure mode of the tests in the database B1 is known, we proposed in this study two kinds of analyses. The first group of analyses investigates the accuracy of different effective shear width models combined with the CSDT model using a database with the governing failure mode known (one-way shear – Database B1). From these analyses, we derive recommendations for the assessment of existing structures when the governing failure mode is known (one-way shear), and precise estimation of the shear capacity is the main purpose.

The second group of analyses aims to assess the shear capacity of slabs when the governing failure mode is unknown (Database B0). This means that one-way or two-way shear failures were included in the analyses. In order to provide consistent predictions of shear capacity regardless of the critical failure mode and covering different support conditions, the General Effective Shear width model (GEWS) was developed accounting that if punching failure governs, the predicted one-way shear capacity should be decreased by predicting a smaller effective shear width.

The idea of the GESW model is to provide a simple alternative to assess the shear capacity of slabs using only a one-way shear model combined with an effective shear width. The proposed model is based on the French effective shear width model [32] adjusted by a correction factor α. This factor considers that increasing the shear slenderness ($\lambda = M/Vd$) or decreasing the effective depth of the reinforcement, the punching shear failure becomes governing. Therefore, a reduced effective shear width should be predicted for slabs on which punching shear may be critical. The values of α were derived based on regression analyses to improve the average and coefficient of variation of the ratio V_{exp}/V_{calc} with the CSDT model combined with the French model of effective shear width. These regression analyses were organized according to the support conditions of the tests (Figure 10).

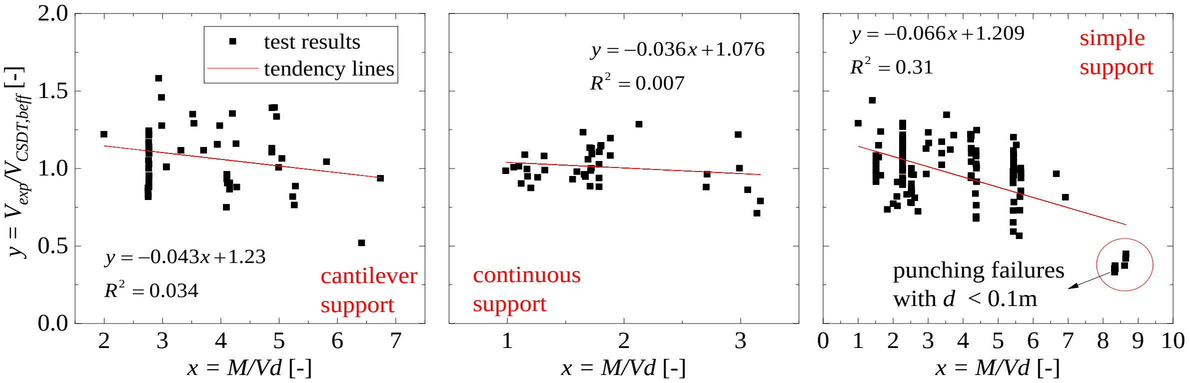

Figure 10 - Ratio of V_{exp} / V_{cal} of the CSDT combined with the original French effective shear width model and $\beta_{proposed}$ to account improved arching action for loads close to the support.

Based on the literature review (Section 2) and parameters influence of V_{exp}/V_{cal} according to the Database B0 similar to showed in Figure 10, we identified that the shear slenderness parameter *M/Vd* would be the most important parameter to be considered in the GESW for all support conditions. Table 4 shows the equations for the proposed model of effective shear width. Figure 8a and Figure 11 illustrates this idea for simply supported slabs of small thickness. In Table 4, we considered the effective depth *d* only for simply supported members by two reasons: (i) the thickness variation is small in the database for other support conditions and (ii) to improve the predictions of tests with punching failure and effective depth lower than 0.1 m (Figure 10). At this point, we highlighted that this approach seeks to provide a model for design or preliminary assessment of existing structures. When higher levels of approximation are required, the use of one-way and two-way shear models is essential to determine the governing failure mode, as we will discuss in the next sections.

Table 4 - General effective shear width model proposed (GESW) according to the support conditions, shear slenderness $\lambda = M/Vd$, and effective depth *d* of the longitudinal reinforcement.

General model	$b_{GESWM} = b_{eff,French} \cdot \alpha$	(42)
Cantilever slabs	$b_{GESWM} = b_{eff,French} \cdot (-0.05 \cdot \lambda + 1.05)$	(43)
Simple support	$b_{GESWM} = b_{eff,French} \cdot \left[(0.31 \cdot d - 0.103) \cdot \lambda + 1.08\right]$	(44)
Continuous support	$b_{GESWM} = b_{eff,French} \cdot (-0.072 \cdot \lambda + 1.08)$	(45)

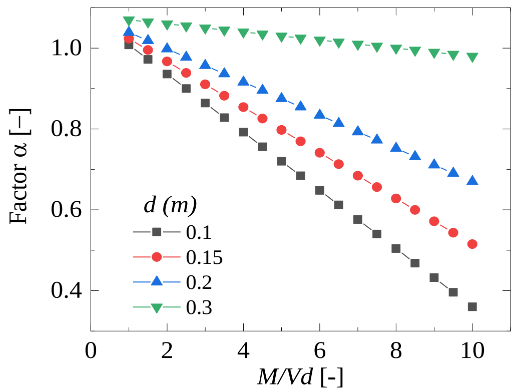

Figure 11 – Variation of the factor α according to the shear slenderness and effective depth of reinforcement for the simply supported slabs.

5 RESULTS

This section addresses a comparison between the experimental shear strengths from the databases A, B0, B1 and C [62], and those predicted by the CSDT model. Firstly, the level of accuracy (average value - AVG) and precision (coefficient of variation - COV) of the V_{exp}/V_{cal} ratio for a database of wide members loaded over the entire width was assessed according to the shear slenderness, with no influence of the effective shear width model (Database A -Section 5.1). In a second step, the analyses involved the database of slabs under single concentrated loads failing in one-way shear (Database B1 - Sections 5.2, 5.3 and 5.4). Then we compared the predicted one-way shear capacities with the experimental ones for 8 tests of slabs subjected to double concentrated loads parallel to the support (Database C - Section 5.5). Finally, we discuss the results of analyses conducted for the overall database of slabs under single loads (Database B0- Sections 5.6) using one-way and two-way shear models.

5.1 Members loaded over the full width – Proposal for $\beta_{arching}$

This analyses aims to assess only the proposed model regarding the improved arching action for non-slender members, without the influence of the effective shear width models. For this study, a database of wide beams and one-way slabs loaded over the entire was used (Database A). This database is published in the public domain [62] and covers different support conditions and a comprehensive range of shear slendernesses. The database includes 36 tests with $M/Vd \leq 2.5$ and 146 tests with $M/Vd > 2.5$.

Figure 12 shows a β factor derived based on a regression analysis with exponential adjustment according to the shear slenderness $\lambda = M/Vd$. This graph highlighted that the scatter between predicted and calculated shear strengths in the range of shear slenderness lower than 3 is considerably higher compared to the other range. This occurs because the arching action is highly influenced by the cracking pattern, which shows a higher variability for short slenderness [57]. Since the CSDT model already takes into account the shear slenderness by the calculations of M_{Ed} and V_{Ed}, the β factor based on the ratio M/Vd could lead to overly optimistic predictions of resistance, mainly when arching action does not play an influence as a result of the occurring cracking pattern (see test without arching action in Figure 12). Because of this, some authors proposed to adopt the inclined cracking load instead of the ultimate shear load as the failure criterion since this parameter shows a considerably lower scatter [57]. However, as most references do not report the inclined cracking load for slab tests as this cracking is harder to observe in slabs under concentrated loads than in beam members, the ultimate shear load was considered in the regression analyses.

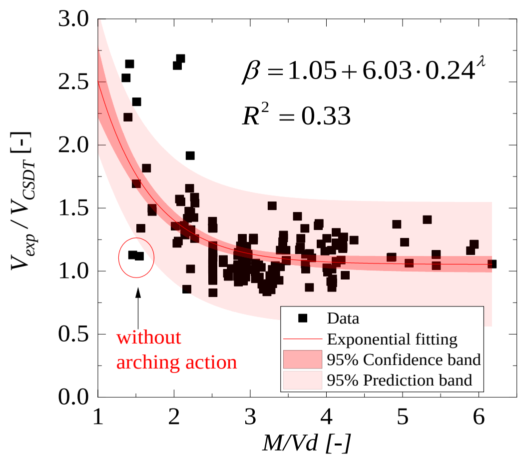

Figure 12 – Alternative β factor derived based on exponential fitting between experimental and predicted shear strengths. Note: λ = *M/Vd*.

Figure 13 shows the V_{exp}/V_{calc} ratio according to the shear slenderness by including or not different approaches for improved arching action for non-slender members. The gray ranges represent ±1 standard deviation from the mean value.

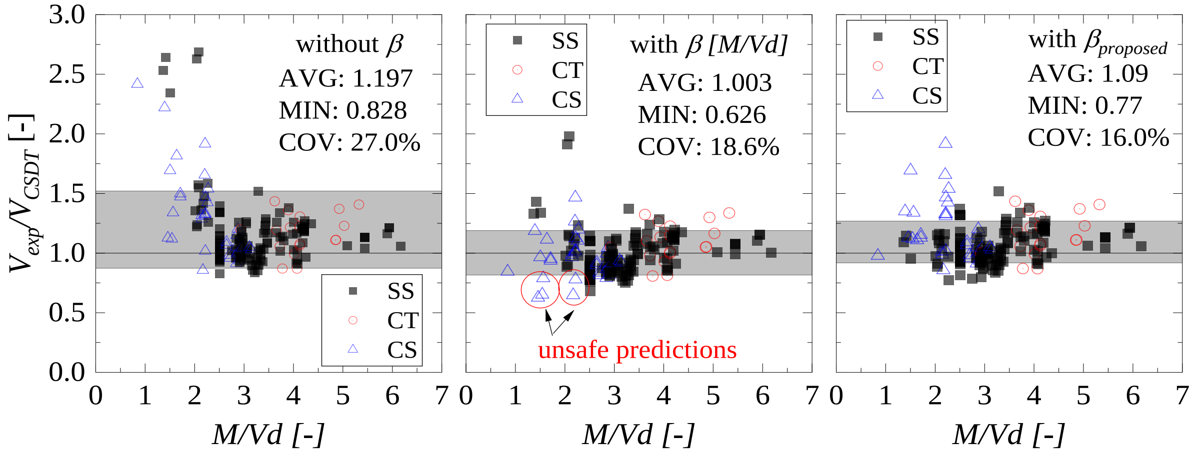

Figure 13 - Effect of factor β on the statistics of V_{exp}/V_{cal} for tests loaded over the entire width (line loads). (CS = continuous support; CT = cantilever support and SS = simple support).

According to Figure 13, applying an improved arching action factor with the CSDT reduces the coefficient of variation from 24.7% to 18.6% when using β*[M/Vd]* (Figure 12), and to 16.0% when using $\beta_{proposed}$ (Equation (41)). Any approach shows a wider scatter between experimental and predicted shear capacities for continuous members (CS), due to the higher variability in the position of the critical shear crack. Although the theoretical critical section was at *d/2* from the position with the maximum bending moment, this procedure is still conservative for most tests. Table 5 shows that the average (AVG) V_{exp}/V_{cal} ratio ranged from 1.197 to 1.093 with the proposed factor β_{prop}. In Table 5, $V_{exp,red}$ refers to the experimental shear capacity reduced by the different parameters β. The lower scatter between experimental and predicted shear capacities occurred with the $\beta_{proposed}$ and β_{EC}.

Table 5 - Statistical results of the predicted to calculated shear strengths according to different approaches to account the arching action for non-slender members.

	$\frac{V_{\exp}}{V_{CSDT}}$	$\frac{V_{\exp,red}}{V_{CSDT}}$	$\frac{V_{\exp,red}}{V_{CSDT}}$	$\frac{V_{\exp,red}}{V_{CSDT}}$
Approach	*Without* β	*With* β_{EC}	*With* $\beta_{\text{Figure 12}}$	With β_{proposed}
AVG	1.197	1.134	1.003	1.093
MIN	0.828	0.828	0.626	0.770
COV	0.270	0.172	0.186	0.160

5.2 Effective shear width models

The database B1 gathered according to the descriptions in Section 3 [62] was used in the next analyses of the level of accuracy of the CSDT combined with different approaches for the effective shear width. Table 6 and Table 7 show statistical results from the V_{exp}/V_{calc} ratio for different ranges of shear slenderness $\lambda=M/Vd$. The results are shown as a function of the ratio M/Vd instead of the ratio a_v/d since the former is a more useful parameter to distinguish members subjected to shear-compression failure from those subjected to flexure-shear failures, mainly for continuous slabs. $\beta_{proposed}$, which accounts for improved arching action for non-slender members, was adopted in most analyses. Since some tests did not fulfill conditions related to load dimensions for use the effective width from the German guidelines [39], Equations (6) to (10) in Table 1, this model was not evaluated. In the same way, the model provided by Halvonik et al. [15] was not evaluated since this was purposed only for cantilever specimens.

According to Table 6, older design code models of effective shear width, such as the Brazilian model [30], lead to overly conservative predictions in most cases (mean $V_{exp,red}/V_{CSDT}$ = 1.772). The Swedish provisions [40], on the other hand, lead to unsafe predictions, with average ratios of V_{exp}/V_{cal} of 0.706 and 0.981 in the different ranges of shear slenderness evaluated. The *fib* model of effective shear width leads to average values of V_{exp}/V_{cal} of 1.092 and 1.192 for non-slender and slender members, respectively. The best accuracy and precision over the different slenderness ranges assessed were achieved by the French model of effective shear width [32], thus indicating, on average, that the French approach provides reasonable predictions of effective shear width for slabs failing in one-way shear.

Table 6 - Statistics of V_{exp}/V_{calc} according to the range of shear slenderness λ = *M/Vd* and effective width model provided in design codes.

			$\frac{V_{\exp,red}}{V_{CSDT}}$	$\frac{V_{\exp,red}}{V_{CSDT}}$	$\frac{V_{\exp,red}}{V_{CSDT}}$	$\frac{V_{\exp,red}}{V_{CSDT}}$
		b_{eff}	**ABNT**	**Swedish**	**French**	***Fib***
λ	**N**	$\beta_{arching}$	**Prop**	**Prop**	**Prop**	**Prop**
<2.5	55	AVG	1.401	0.706	1.044	1.092
		MIN	0.869	0.481	0.773	0.758
		COV	21.9%	23.5%	11.4%	20.8%
≥2.5	86	AVG	2.009	0.981	1.070	1.192
		MIN	0.818	0.438	0.723	0.513
		COV	40.8%	18.7%	15.8%	23.7%
All	141	AVG	1.772	0.873	1.060	1.153
		MIN	0.818	0.438	0.723	0.513
		COV	41.2%	25.4%	14.3%	23.0%

Table 7 - Statistics of V_{exp}/V_{calc} according to the range of shear slenderness λ = *M/Vd* and effective width models suggested in the literature.

			$\frac{V_{\exp,red}}{V_{CSDT}}$	$\frac{V_{\exp}}{V_{CSDT}}$	$\frac{V_{\exp,red}}{V_{CSDT}}$	$\frac{V_{\exp,red}}{V_{CSDT}}$
		b_{eff}	**Zheng**	**Reissen**	**Bauer**	**Prop (GESW)**
λ	**N**	$\beta_{arching}$	**Prop**	**-**	**Prop**	**Prop**
< 2.5	55	AVG	0.755	1.601	1.401	1.043
		MIN	0.512	1.113	0.869	0.748
		COV	22.7%	17.7%	21.9%	12.2%
≥ 2.5	86	AVG	1.302	1.638	2.009	1.295
		MIN	0.459	0.983	0.818	0.830
		COV	34.0%	29.6%	40.8%	19.2%
All	141	AVG	1.089	1.624	1.772	1.197
		MIN	0.459	0.983	0.818	0.748
		COV	41.3%	25.7%	41.2%	20.3%

Table 7 shows that the average value of V_{exp}/V_{cal} ranged from 1.089 to 1.772 with the approaches studied for the definition of an effective shear width. The effective width from Zheng et al. [41] provided a wider scatter between experimental and predicted shear capacities (COV > 30% on average) and a V_{exp}/V_{cal} mean value much lower than 1 for non-slender members. Since the approach of Reiβen [21] includes the effect of the improved arching action on non-slender members in the effective width model by using the factor k_{bf} (Equation (21) in Table 1), the experimental shear capacities were not reduced for these calculations. The model provided conservative predictions of shear strength for all tests assessed and a 25.7% coefficient of variation. Bauer and Muller's approach [83] resulted in the most conservative predictions for slender members (V_{exp}/V_{cal} = 2.009), but with a wider scatter (COV = 40.8%). The proposed GESW model provided good AVG (1.197) and COV (20.3%) values compared to the other models. Comparing Table 6 and Table 7, both GESW model and French model provide an accurate estimation of the test results. However, the GESW turns out to be slightly more conservative for Database B1 as it was derived to assess slabs under both failure modes (one-way shear and two-way shear).

5.3 Sensitivity of parameters

Since the first purpose is to derive recommendations for precise predictions of shear strength when the one-way shear failure mode is governing (Database B1), the CSDT combined with the French effective shear width model and β_{prop} was further assessed with parameter studies (Figure 14).

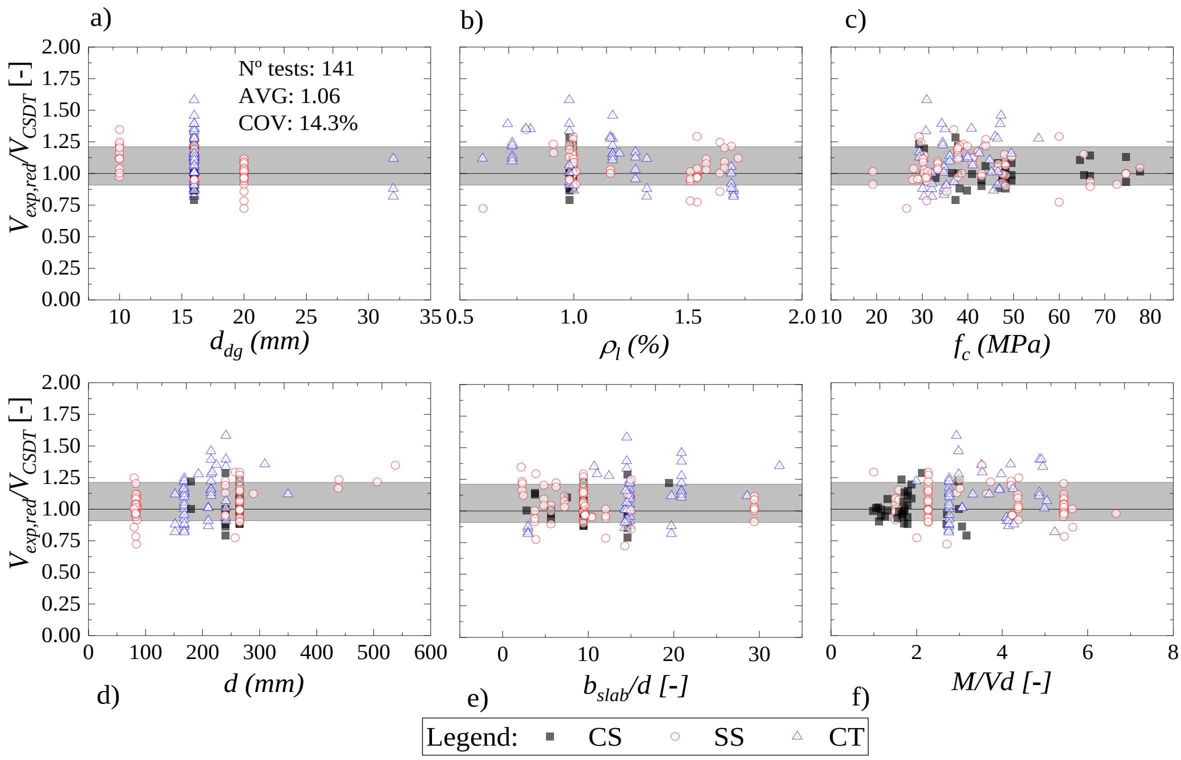

Figure 14 - V_{exp}/V_{cal} ratio as a function of the main mechanical and geometrical parameters for wide members subjected to concentrated loads close to the support with predominant one-way shear failure: a) aggregate size d_g, b) longitudinal reinforcement ratio ρ_l, c) concrete compressive strength f_c, d) effective depth d, e) width-to-effective depth ratio b/d, and (e) shear slenderness M/Vd. (CS = continuous support; CT = cantilever support and SS = simple support).

Figure 14 shows the ratio of $V_{exp,red}/V_{cal}$ as a function of different parameters. The results indicate no significant influence of the aggregate size (Figure 14a) and reinforcement ratio (Figure 14b) on the predictions of shear strength with the studied approach. Wider scatter in some regions (see Figure 14a) for 16 mm aggregate size can be assigned to a higher number of tests. Figure 14c shows that the CSDT provides accurate and precise predictions of shear strength for members of high strength concrete ($f_c > 65$ MPa), for which a lower contribution of the aggregate interlock is accounted for by the parameter R_{ai} from the CSDT. This approach also handled well the range of thicknesses studied (Figure 14d). Although the range of thickness studied is not representative of solid slab bridges [10], the available results are of interest for slab-between-girders bridges. Moreover, the studied approach enabled accurate predictions, regardless of the shear slenderness parameter *M/Vd* (Figure 14f).

5.4 Comparison with design code provisions

Table 8 shows a comparison of different code-based approaches for the one-way shear capacity of the experiments gathered in database B1 described in Section 3. The French model is used for determining the effective width in combination with code provisions from Europe [50,56] and North America [84]. The *fib* Model Code 2010 [34] is the only code which includes guidance for improved arching action and effective width for concentrated loads close to the support. The same factor β_{prop} for use with the CSDT was adopted in combination with the Swiss code SIA 262:2013 model [56] and with the AASHTO code provisions for bridges [84].

Table 8 - Statistics of V_{exp}/V_{calc} according to the range of shear slenderness λ= *M/Vd* for different design code approaches.

			$\frac{V_{\exp,red}}{V_{CSDT}}$	$\frac{V_{\exp,red}}{V_{CSDT}}$	$\frac{V_{\exp,red}}{V_{AASHTO}}$	$\frac{V_{\exp,red}}{V_{CEN04}}$	$\frac{V_{\exp,red}}{V_{MC}}$	$\frac{V_{\exp,red}}{V_{SIA262}}$
		b_{eff}	**French**	**GESW**	**French**	**French**	***fib* MC**	**French**
λ	**N**	$\beta_{arching}$	**Prop**	**Prop**	**Prop**	**CEN (2005)**	***fib* MC**	**Prop**
		AVG	1.044	1.043	1.421	1.704	1.762	1.096
		MIN	0.773	0.748	0.986	1.095	1.176	0.819
<2.5	55	COV	11.4%	12.2%	16.5%	18.0%	22.6%	14.8%
		AVG	1.070	1.295	1.476	1.122	1.479	1.037
		MIN	0.723	0.830	0.918	0.606	0.749	0.733
>2.5	86	COV	15.8%	19.2%	33.3%	24.0%	29.0%	16.4%
		AVG	1.060	1.197	1.454	1.349	1.589	1.060
		MIN	0.723	0.748	0.918	0.606	0.749	0.733
All	141	COV	14.3%	20.3%	28.2%	29.8%	27.6%	15.9%

Table 8 shows that the code provisions studied provided a mean ratio of V_{exp}/ V_{cal} between 1.043 and 1.704 for λ < 2.5. The most precise results were achieved by the French effective shear width model combined with the one-way shear model based on the CSDT, as proposed in this study when the governing failure mode is known and is one-way shear. The predictions with the AASHTO code provisions were more conservative, with a mean ratio between experimental and calculated shear strengths higher than 1.4 on both ranges of shear slenderness studied.

Table 8 also shows that the average ratio of V_{exp}/V_{cal} ranged from 1.060 to 1.589 for a shear slenderness higher than 2.5. Remarkably, the Swiss code provisions reached the same level of accuracy and precision of CSDT when combined with the French model of effective shear width and use of β_{prop}. Although these models (CSDT and SIA 262:2013) were derived in different ways, this result occurs because both models rely on some similar ideas, such as the higher influence of aggregate interlock in the shear strength and the decrease of the shear strength for increasing shear slenderness. Since both AASHTO models and *fib* Model Code Models were derived based on the Simplified Modified Compression Field Theory (SMCFT [78]), the statistical differences can be attributed to the models to account for improved arching action and the effective shear width used.

5.5 Test with double loads

The number of tests with double loads parallel to line supports is very limited. There are only 8 tests in the literature conducted by Rombach and Henze [85], Vaz Rodrigues et al. [19] and Reiβen et al. [3]. Most of these tests were conducted on cantilever slabs (7/8). The test with 4 loads close to the line support conducted by Vaz Rodrigues [19] showed a punching failure and was not analyzed in this study because it showed a transitional failure between the one-way and two-way shear. Table 9 shows the statics of the ratio between experimental and predicted one-way shear resistances for these tests. In summary, the level of accuracy of the CSDT model combined with the French effective shear width was close to that of slabs subjected to a single load. However, additional tests are needed to confirm these findings. The most unsafe prediction in Table 9 (V_{exp}/V_{pred} = 0.89) occurred for the only test with a ratio $a_v/d < 2.5$. Therefore, the proposed factor to consider arching action (β_{prop}) may have been too optimistic for this type of loading.

Table 9 - Statistical of the experimental to calculated shear strengths for tests with double loads close to a line support.

Authors	Test	$\frac{V_{\exp,red}}{V_{CSDT,beff\ \text{French}}}$
Vaz Rodrigues et al [19]	DR1b	1.26
	DR2a	1.03
	DR2b	1.07
Rombach & Henze [85]	2*d* x 2	0.89
	3*d* x 2	0.99
	4*d* x 2	1.06
	5*d* x 2	1.01
Reiβen et al. [3]	MS35BB-22	1.04
	AVG	1.04
	COV (%)	9.78

5.6 General approach for one-way and two-way shear

An alternative approach to assessing the one-way shear models applicable to members with possible punching failure is to decrease the effective shear width accordingly with the shear slenderness, as discussed in the proposed GESW model (Section 4). In this study, we assumed that the French effective shear width should be multiplied by the parameter α (Equation (42)).

Table 10 shows the statistics of the ratio between experimental and predicted shear capacities with one-way and two-way shear models according to the failure mode for the database with 214 test results of slabs under single concentrated loads (Database B0). For the punching shear provisions, the proposed model from prEN 1992-1-1:2018 [86] was used (based on the CSCT), while for the one-way shear models we combined the CSDT models with the French and GESW models. Table 10 shows that the level of precision reached with the CSDT combined with the GESW model is very similar for both failure modes, while the other approaches provide precise estimations only for their respective failure modes.

Table 10 - Comparison of predictions with the CSDT for one-way shear and the punching shear provisions from prEN 1992-1-1:2018 [86] according to the failure mode.

Failure mode	Nº		$\frac{P_{\exp}}{P_{EC18}}$	$\frac{V_{\exp,red}}{V_{CSDT}}$	$\frac{V_{\exp,red}}{V_{CSDT}}$
		b_{eff}	-	French	GESW
P	51	AVG	1.092	0.808	1.044
		MIN	0.724	0.331	0.712
		COV	20.0%	31.6%	21.2%
WB	141	AVG	1.219	1.060	1.197
		MIN	0.466	0.723	0.748
		COV	31.9%	14.3%	20.3%
WB/P	22	AVG	1.220	1.007	1.121
		MIN	0.942	0.712	0.833
		COV	21.5%	13.4%	15.6%
All	214	AVG	1.189	0.994	1.153
		MIN	0.466	0.331	0.712
		COV	29.2%	21.0%	20.8%

6 DISCUSSIONS

Previous publications on the field of one-way slabs under concentrated loads usually concentrate on the accuracy of semi-empirical models applied to reduced databases [10,11]. When mechanical-based models are investigated, usually the analyses concentrate on one kind of support condition [15]. Most of them neglect the governing failure mode of the tests [11,87]. Therefore, a gap of more comprehensive studies is realized related to the shear capacity of slabs under concentrated loads failing in different modes.

Tests with a presumed punching failure were initially removed from the database B1. Only members with predominant one-way shear failure were used in the first statistical analyses. Therefore, part of the higher level of accuracy in Section 5.2 with the French effective shear width can be attributed to the improved database selection. However, we have highlighted that the classification of the failure modes for some members may not be an easy task. For such cases, the experiments must be classified as governed by a mixed failure between one-way shear and two-way shear, as made in previous publications [10]. In these tests, both conical cracks at the top/bottom face and flexure-shear cracks at the edges of the slab arise at failure. Some studies have claimed that one-way and two-way shear capacities can be very similar is terms of strength ratio (V_{exp}/V_{calc} similar to P_{exp}/P_{calc}) [20], which was also verified in this study for some tests during the classification of the failure modes. Particularly, this is also in line with the ACI 318-19 punching provisions [88], where the punching capacity is assumed to be governed by one-way shear when the load becomes very rectangular.

Since most mechanical models, such as the CSDT [6], CSCT [77], and SMCFT [78] were derived from flexure-shear failures, one could question their possible extension to non-slender members, whose predominant failure mode is a shear-compression failure. In fact, some studies, as well as the current ACI 318-19 [88], have highlighted those members should be assessed by strut-and-tie models, instead of sectional strain-based models [89,90]. However, most engineers have raised the possibility of covering a more extensive range of cases with the same model. In particular, for the shear assessment of existing RC slab bridges, there is a need for uniform approaches that allow checking all cross-sections and load positions in a preprogrammed way. Such an approach requires the checking of models for non-slender members in an approach similar to the one suggested in design guides, e.g., NEN 1992-1-1:2005 [50] and *fib* Model Code 2010 [34], i.e. based on the reduction of the acting shear load close to the support. We have highlighted that such analyses should be used only as a first assessment of structures without stirrups. As such, they are in line with the need for a preprogrammed method for the assessment of a large number of existing RC slab bridges.

The level of accuracy reached by the CSDT with our method for arching action and the French model of effective width is similar to that obtained by the CSCT [2], but removes the need for finite element calculations. The proposed CSDT extension excels due to its easy application. The overall V_{exp}/V_{cal} average ratio with the CSDT is 1.06, with a 14.3% coefficient of variation for a set with 141 test results. Comparatively, Natário [2] achieved a 1.12 V_{exp}/V_{calc} average ratio with 11% COV for simply supported members (62 tests) and 1.07 AVG and 16% COV for cantilever members (27 tests). However, Natário's study did not include continuous members or members with combinations of loads (concentrated loads combined with line loads). The database B0 has 33 tests with loads close to continuous supports. The mean ratio between experimental and predicted shear capacities by the CSDT model with the French effective shear width and β_{prop} is 1.01 with a COV of 11.3%. Therefore, this study comprehends a larger variety of support and loading conditions. The narrow scatter between experimental and predicted shear capacities with the CSDT demonstrates its accuracy and precision in assessing the one-way shear capacity of wide RC members under concentrated loads, such as slab bridges.

Different from other studies [15,28], we have identified that the use of the French approach for determining the effective shear width provides reasonable levels of accuracy combined with the one-way shear strength model based on the CSDT. Regarding studies on simply supported members in which the French model leads to unsafe predictions of the shear strength [15,28], our analysis indicates that these experiments presented signals of punching failures and, therefore, should also be evaluated by two-way shear strength models to reach more precise predictions.

Notably, the CSDT combined with the GESW model provides homogeneous levels of precision in predicting the shear capacity for specimens with one-way and two-way shear failures in the database B0, capturing well the complex transition between these two failure modes. The reason for this observation is that the precision and accuracy of the predictions with the GESW model were similar between different failure modes, shear slenderness, and support conditions. In addition, the level of precision was considerably better than that obtained with current semi-empirical code models [10,87], for which COVs are usually larger than 35%. Therefore, in a programmed approach of assessment, the CSDT combined with the GESW model may be used as the only model to check shear failures when the governing failure mode is unknown.

7 CONCLUSIONS

This study presents an extension of the Critical Shear Displacement Theory model for wide members under concentrated loads. Different databases were used to assess (i) the proposed arching action factor, (ii) the accuracy and precision of the CSDT combined with different models of effective shear width for slabs under single concentrated loads; (iii) the accuracy of the CSDT model to assess members with double concentrated loads parallel to the support and (iv) to assess slabs that showed different failures modes in shear. The following can be concluded:

1. The model for improved arching action for non-slender members can be combined with the CSDT as a first step for the determination of their shear strength. This approach was validated against databases of wide members loaded over the entire width, as well as for slabs under concentrated loads failing in one-way shear.

2. The CSDT, combined with the effective width model from the French design guides [32], provides accurate results of shear strength for wide members with predominant one-way shear failure, regardless of the shear slenderness and support conditions. The same level of precision was reached for slabs under double concentrated loads parallel to the support.

3. The level of accuracy of our proposed approach based on the CSDT combined with the French effective shear width was higher than that of most design code models, regardless of the parameters analyzed. Since our approach requires only analytical calculations (without finite element analysis), it can easily be implemented in the daily engineering practice for first levels of approximation.

4. Despite the simplicity of the French effective width model, it seems to represent well most one-way shear tests investigated. However, for members with punching failure, the approach may lead to unsafe predictions of shear strength, as verified in this study. Since the governing failure mode may not be known in preliminary analyses, both failure modes must be checked in the daily engineering practice for higher levels of approximation.

5. The most general effective shear width model (GESW) leads to good levels of accuracy for slabs under concentrated loads since it deals with both one-way and two-way shear failures. Moreover, the proposed approach addresses in a novel manner the transition between one-way shear and two-way shear failures of slabs under concentrated loads. However, it should be highlighted that this approach should be used only for preliminary designs and global assessment of a large number of assets, since it does not determine the governing failure mode physically. Apart from that, further studies are required in order to include the effects of other parameters, such as the slab width *b* in the transition between one-way and two-way shear failures.

6. This study shows that traditional models of effective shear width and punching shear do not provide precise predictions of shear strength when the critical failure mode is other than that assumed by the model (Section 5.6). Because of this, adjustments are required on each model to extend the applications of them for both failure modes. In this study, different approaches are shown to assess the shear capacity when the governing failure mode is known or unknown. The proposed approaches apply to wide beams and slabs under different support conditions (simple, continuous, and cantilever support), different loading conditions (loaded over the entire width or concentrated on the width direction).

DECLARATION OF CONFLIT INTEREST

The authors declare that they have no known competing financial interest or personal relationships that could have appeared to influence the work reported in this paper.

CREDIT AUTHORSHIP CONTRIBUTION STATEMENT

Alex de Sousa: Conceptualization, Methodology, Resources, Data curation, Writing - original draft, preparation. Eva Lantsoght: Conceptualization, Supervision, Writing - review & editing. Yuguang Yang: Supervision, Writing - review & editing. Mounir El Debs: Supervision, Project administration, Funding acquisition & manuscript review.

ACKNOWLEDGMENTS

The authors acknowledge the financial support provided by the Brazilian National Council for Scientific and Technological Development (CNPq) and the São Paulo Research Foundation (FAPESP 2018/21573-2 and FAPESP 2019/20092-3) and Angela Pregnolato Giampedro for the English language revision.

Notation	Description
a	shear span: distance between the center of the support and the center of the load
a_v	clear shear span: distance between face of support and face of load
b	width of the structural member
b_n	clear width of the structural member
d	effective depth of longitudinal reinforcement
d_t	effective depth of transverse reinforcement
d_g	maximum aggregate size
f_c	concrete compressive strength
f_{ck}	characteristic concrete compressive strength
f_{cm}	mean value of cylinder compressive strength of concrete
f_y	yield strength of reinforcement
k_c	slope of stress line, k_c = 1.28 according to [91]
m_{Ed}	design (factored) moment per unit length in critical section
m_{Rd}	plastic design (factored) moment per unit length in critical section
n_e *or* n	ratio between elastic modulus of steel and concrete
$l_{cr,m}$	spacing of two neighboring major cracks
$s_{cr,CSDT}$	height of fully developed crack
s_{rm}	crack spacing of primary cracks
w	crack width
w_b	crack width at the bottom of the crack
x	neutral axis depth
z	length of internal level arm or effective shear depth according to *fib* MC 2010, taken as 0.9*d*
A_x, A_y	projected areas of a cracked surface for a unit crack length in two directions
A_s	longitudinal reinforcement area
A_g	gross area of concrete section
E_c	modulus of elasticity of concrete
E_s	elastic modulus of steel
G_c	modulus of shear deformation for un-cracked concrete chord
G_f	concrete fracture energy
M	cross-sectional bending moment
M_{Ed}	design sectional moment
N_{Ed}	design sectional axial load
P_{exp}	measured peak load in an experiment
P_{EN18}	Predicted punching capacity by prEN 1992-1-1:2018 [86]
V	shear force
V_{ai}	shear force transferred by aggregate interlock
V_c	shear force transferred in concrete compression zone
V_d	shear force transferred by dowel action
V_{Ed}	design shear force
V_{exp}	Experimental shear force strength from the database tests
$V_{exp,red}$	Experimental shear force reduced by the parameter β
V_{cal}	Calculated shear force strength
V_{AASHTO}	one-way shear capacity calculated according to AASHTO
V_{CEN}	one-way shear capacity calculated according to NEN 1992-1-1:2005
V_{ACI-19}	one-way shear capacity calculated according to ACI 318-19
V_{MC}	one-way shear capacity calculated according to Model Code 2010

V_{SIA}	one-way shear capacity calculated according to SIA 262:2013
V_{CSDT}	one-way shear capacity calculated according to CSDT
α_e	modular ratio (E_s/E_c)
β	reduction factor for the contribution of loads close to the support to the shear force
γ_c	partial safety factor for concrete
Δ	shear displacement at crack
Δ_{cr}	critical shear displacement
Δ_e	distance between neutral axis and center of internal lever arm z
ε_s	steel strain
ε_x	longitudinal strain at mid-depth of the effective shear depth
ϕ	rebar diameter
$\mu_{,CSDT}$	friction coefficient for contact area between aggregate particles and matrix with $\mu = 0.4$ proposed according to Walraven [92]
ρ_s	longitudinal reinforcement ratio
σ	normal stress
σ_{pu}	crushing (yielding) strength of matrix, or contact stress at cracked surface
τ	shear stress
τ_{ai}	shear stress transferred by aggregate interlock
τ_{Rd}	design shear capacity of concrete
τ_c	concrete shear capacity
AVG	Average value
COV	coefficient of variation
CSCT	Critical Shear Crack Theory
CSDT	Critical Shear Displacement Theory
SMCFT	Simplified Modified Compression Field Theory
MIN	Minimum value

REFERENCES

[1] Lantsoght EOL, Van Der Veen C, Walraven JC. Shear in One-Way Slabs under Concentrated Load Close to Support. ACI Struct J 2013;110.

[2] Natário F, Fernández Ruiz M, Muttoni A. Shear strength of RC slabs under concentrated loads near clamped linear supports. Eng Struct 2014;76:10–23. https://doi.org/10.1016/j.engstruct.2014.06.036.

[3] Reiβen K, Classen M, Hegger J. Shear in reinforced concrete slabs-Experimental investigations in the effective shear width of one-way slabs under concentrated loads and with different degrees of rotational restraint. Struct Concr 2018;19:36–48. https://doi.org/10.1002/suco.201700067.

[4] Henze L, Harter M, Rombach GA. Querkrafttragfähigkeit von Stahlbetonplatten ohne Querkraftbewehrung unter konzentrierten Einzellasten (Shear capacity of reinforced concrete slabs without transverse reinforcement under concentrated loads Part 2: Proposal for a new design model). Beton- Und Stahlbetonbau 2019. https://doi.org/10.1002/best.201800106.

[5] de Sousa AMD, Lantsoght EOL, El Debs MK. One-way shear strength of wide reinforced concrete members without stirrups. Struct Concr 2020:1–25. https://doi.org/10.1002/suco.202000034.

[6] Yang Y, den Uijl J, Walraven J. Critical shear displacement theory: on the way to extending the scope of shear design and assessment for members without shear reinforcement. Struct Concr 2016;17:790–8. https://doi.org/10.1002/suco.201500135.

[7] Yang Y, Walraven J, Uijl J den. Shear Behavior of Reinforced Concrete Beams without Transverse Reinforcement Based on Critical Shear Displacement. J Struct Eng 2017;143:04016146. https://doi.org/10.1061/(ASCE)ST.1943-541X.0001608.

[8] Gurutzeaga M, Oller E, Ribas C, Cladera A, Marí A. Influence of the longitudinal reinforcement on the shear strength of one-way concrete slabs. Mater Struct Constr 2015;48:2597–612. https://doi.org/10.1617/s11527-014-0340-5.

[9] Conforti A, Minelli F, Plizzari GA. Influence of width-to-effective depth ratio on shear strength of reinforced concrete elements without web reinforcement. ACI Struct J 2017;114:995–1006. https://doi.org/10.14359/51689681.

[10] Lantsoght EOL, van der Veen C, Walraven JC, de Boer A. Database of wide concrete members failing in shear. Mag Concr Res 2015;67:33–52. https://doi.org/10.1680/macr.14.00137.

[11] Henze L, Rombach GA, Harter M. New approach for shear design of reinforced concrete slabs under concentrated loads based on tests and statistical analysis. Eng Struct 2020;219:110795. https://doi.org/10.1016/j.engstruct.2020.110795.

[12] Reiβen K, Hegger J. Experimentelle Untersuchungen zum Querkrafttragverhalten von auskragenden Fahrbahnplatten unter Radlasten. Beton- Und Stahlbetonbau 2013;108:315–24. https://doi.org/10.1002/best.201200072.

[13] Reißen K, Hegger J. Experimentelle Untersuchungen zur mitwirkenden Breite für Querkraft von einfeldrigen Fahrbahnplatten. Beton- Und Stahlbetonbau 2013;108:96–103. https://doi.org/10.1002/best.201200064.

[14] Lantsoght EOL, van der Veen C, Walraven J, de Boer A. Experimental investigation on shear capacity of reinforced concrete slabs with plain bars and slabs on elastomeric bearings. Eng

Struct 2015;103:1–14. https://doi.org/10.1016/J.ENGSTRUCT.2015.08.028.

[15] Halvonik J, Vidaković A, Vida R. Shear Capacity of Clamped Deck Slabs Subjected to a Concentrated Load. J Bridg Eng 2020;25:04020037. https://doi.org/10.1061/(ASCE)BE.1943-5592.0001564.

[16] Bui TT, Abouri S, Limam A, NaNa WSA, Tedoldi B, Roure T. Experimental investigation of shear strength of full-scale concrete slabs subjected to concentrated loads in nuclear buildings. Eng Struct 2017;131:405–20. https://doi.org/10.1016/j.engstruct.2016.10.045.

[17] Lantsoght EOL, van der Veen C, Walraven JC, de Boer A. Transition from one-way to two-way shear in slabs under concentrated loads. Mag Concr Res 2015;67:909–22. https://doi.org/10.1680/macr.14.00124.

[18] Muttoni A, Fernandez Ruiz M. Shear in slabs and beams: should they be treated in the same way? Fédération Int. du Bét. Bull. N°57, 2010, p. 105–28.

[19] Vaz Rodrigues R, Fernández Ruiz M, Muttoni A. Shear strength of R/C bridge cantilever slabs. Eng Struct 2008;30:3024–33. https://doi.org/10.1016/j.engstruct.2008.04.017.

[20] Natário F. Static and Fatigue Shear Strength of Reinforced Concrete Slabs Under Concentrated Loads Near Linear Support. Thesis (Docteur ès Sciences) - Faculté de L'environnement Naturel, Architectural et Construit Laboratoire de Construction en Béton, École Polytechnique Fédérale de Lausanne, 2015. https://doi.org/10.5075/epfl-thesis-6670.

[21] Reiβen K. Zum Querkrafttragverhalten von einachsig gespannten Stahlbe- tonplatten ohne Querkraftbewehrung unter Einzellasten. PhD Thesis (Doctor of Engineering), Faculty of Civil Engineering, RWTH Aachen University, 2016.

[22] Henze L. Querkrafttragverhalten von Stahlbeton-Fahrbahnplatten. PhD Thesis, Institute for Concrete Structures, Technische Universität Hamburg (TUHH), 2019.

[23] Doorgeest J. Transition Between One-way Shear and Punching Shear. Master of Science Thesis, Delft University of Technology, 2012.

[24] Regan PE. Shear Resistance of Members without Shear Reinforcement; Proposal for CEB Model Code MC90 1987:1–28.

[25] Lantsoght EOL, Van Der Veen C, De Boer A, Walraven JC. Transverse load redistribution and effective shear width in reinforced concrete slabs. Heron 2015;60:145–79.

[26] Lantsoght EOL, de Boer A, van der Veen C. Distribution of peak shear stress in finite element models of reinforced concrete slabs. Eng Struct 2017;148:571–83. https://doi.org/10.1016/j.engstruct.2017.07.005.

[27] Sagaseta J, Tassinari L, Fernández Ruiz M, Muttoni A. Punching of flat slabs supported on rectangular columns. Eng Struct 2014;77:17–33. https://doi.org/10.1016/j.engstruct.2014.07.007.

[28] Reiβen K, Hegger J. Experimental investigations on the effective width for shear. Maintenance, Monit. Safety, Risk Resil. Bridg. Bridg. Networks - Proc. 8th Int. Conf. Bridg. Maintenance, Saf. Manag. IABMAS 2016, 2016, p. 2340–8.

[29] Lantsoght EOL, de Boer A, van der Veen C, Walraven JC. Effective shear width of concrete slab bridges. Proc Inst Civ Eng - Bridg Eng 2015;168:287–98. https://doi.org/10.1680/bren.13.00027.

[30] ABNT NBR 6118. NBR 6118: Design and execution of reinforced concrete buildings (in portuguese). Rio de Janeiro: Associação Brasileira de Normas Técnicas (ABNT); 1980.

[31] NORMCOMISSIE 351001. NEN 6720 Technische Grondslagen voor Bouwvoorschriften 1995.

[32] FD P 18-717. Eurocode 2 - Calcul des structures en béton - Guide d'application des normes NF EN 1992 2013.

[33] Grasser E, Thielen G. Hilfsmittel zur Berechnung der Schnittgrößen und Formänderungen von Stahlbetontragwerken : nach DIN 1045, Ausg. Juli 1988. 3º revised. Berlin: Beuth Verlag GmbH; 1991.

[34] Fédération Internationale du Béton (fib). fib Model Code for Concrete Structures 2010. vol. Vol. 1-2. Lausanne, Switzerland: Ernst & Sohn - fédération internationale du béton, Bulletin 65; 2012.

[35] Bauer T, Müller M. Straßenbrücken in Massivbauweise nach DIN- Fachbericht - Beispiele prüffähiger Standsicherheitsnachweise. 2. Auflage. Berlin: Bauwerk; 2003.

[36] Vidakovi A, Halvonik J. Shear resistance of clamped deck slabs assessed using design equations and FEM analysis. 13th Int. Conf. Mod. Build. Mater. Struct. Tech., 2019, p. 0–7.

[37] Johansen KW. Yield-Line Formulae for Slabs. CRC Press Yea; 2005.

[38] Goldbeck AT. The Influence of Total Width of the Effective Width of Reinforced-Concrete Slabs Subjected to Cental Concentrated Loading. ACI J Proc 1917;13:78–88. https://doi.org/10.14359/15865.

[39] DAfStb. Deutscher Ausschuss für Stahlbeton Heft 240: Hilfsmittel zur Berechnung der Schnittgrößen und Formänderungen von Stahlbetonbauwerken. (German Committee for Structural Concrete Book 240: Tools for calculation of internal forces and changes in shape of rein. Berlin / Germany: Beuth Verlag; 1991.

[40] BBK (Statens Betong Kommitte). Regulations for concrete structures – Part 1: Design. BBK, Stockholm, Sweden; 1979.

[41] Zheng Y, Taylor S, Robinson D, Cleland D. Investigation of ultimate strength of deck slabs in steel-concrete bridges. ACI Struct J 2010;107:82–91.

[42] Reiβen K, Hegger J. Shear Capacity of Reinforced Concrete Slabs under Concentrated Loads. 8th IABSE Congr. 2012 "Innovative Infrastructures - Towar. Hum. Urban., Seoul, Südkorea,: 2012. https://doi.org/10.2749/222137912805111320.

[43] Reiβen K, Hegger J. Numerical investigations on the shear capacity of reinforced concrete slabs under concentrated loads. Res. Appl. Struct. Eng. Mech. Comput., CRC Press; 2013, p. 1507–12. https://doi.org/10.1201/b15963-271.

[44] Rombach GA, Velasco RR. Schnittgrößen auskragender fahrbahnplatten infolge von radlasten nach DIN-fachbericht. Beton- Und Stahlbetonbau 2005;100:376–84. https://doi.org/10.1002/best.200590093.

[45] Shu J, Plos M, Zandi K, Ashraf A. Distribution of shear force: A multi-level assessment of a cantilever RC slab. Eng Struct 2019;190:345–59. https://doi.org/10.1016/J.ENGSTRUCT.2019.04.045.

[46] Kani GNJ. The Riddle of Shear Failure and its Solution. ACI J Proc 1964;61:441–68. https://doi.org/10.14359/7791.

[47] Leonhardt F, Walther R. Schubversuche an einfeldrigen Stahlbetonbalken mit und ohne Schubbewehrung [Shear tests on single-span reinforced concrete beams with and without shear reinforcement]. Berlin: Beuth; 1962.

[48] Cavagnis F, Fernández Ruiz M, Muttoni A. An analysis of the shear-transfer actions in reinforced concrete members without transverse reinforcement based on refined experimental measurements. Struct Concr 2018;19:49–64. https://doi.org/10.1002/suco.201700145.

[49] Bairán JM, Menduiña R, Marí A, Cladera A. Shear Strength of Non-Slender Reinforced Concrete Beams. ACI Struct J 2020:277–90. https://doi.org/10.14359/51721369.

[50] CEN. EN 1992-1-1: Eurocode 2: Design of concrete structures -Part 1-1: General rules and rules for buildings, EN 1992-1-1:2005 2005.

[51] Fernández Ruiz M, Muttoni A, Sagaseta J. Shear strength of concrete members without transverse reinforcement: A mechanical approach to consistently account for size and strain effects. Eng Struct 2015;99:360–72. https://doi.org/10.1016/J.ENGSTRUCT.2015.05.007.

[52] Kim D, Kim W, White RN. Arch Action in Reinforced Concrete Beams—A Rational Prediction of Shear Strength. ACI Struct J 1999;96:586–93. https://doi.org/10.14359/695.

[53] ABNT NBR 6118. NBR 6118: Design of concrete structures — Procedure (in portuguese). Rio de Janeiro: Associação Brasileira de Normas Técnicas (ABNT); 2014.

[54] DIN 1045. Beton und Stahlbeton - Bemessung und Ausführung. Berlin: Deutsches Institut für Normung (DIN); 1988.

[55] DIN 1045-1. Bemessung und Konstruktion von Stahlbeton- und Spannbetonbauteilen. Berlin: Deutsches Institut für Normung (DIN); 2001.

[56] SIA. Code 262 for concrete structures. Zürich: Swiss Society of Engineers and Architects; 2013.

[57] Yang Y, Uijl JA den, Walraven JC. Residual Shear Capacity of 50 years Old RC Solid Slab Bridge Decks. Int. IABSE Conf. Assessment, Upgrad. Refurb. Infrastructures., Rotterdam: 2013, p. 538–9.

[58] Mörsch E. Der Eisenbetonbau [Concrete-steel construction]. New York.: Engineering News Publishing; 1909.

[59] Baumann T, Rusch H. Versuche zum studien der verdübe- lungswirkung der biegezugbewehrung eines stahlbetonbalkens [Exper- imental study on dowel action in reinforced concrete beam]. Deutscher Ausschuss für Stahlbeton (DAfStb), Ernst, Berlin (in German); 1970.

[60] Walraven JC. Fundamental Analysis of Aggregate Interlock. J Struct Div ASCE 1981;107:2245–2270.

[61] Chana PS. Investigation of the mechanism of shear failure of reinforced concrete beams. Mag Concr Res 1987;39:196–204. https://doi.org/10.1680/macr.1987.39.141.196.

[62] Sousa AMD, Lantsoght EOL, El Debs MK. Database of wide beams and slabs under concentrated loads failing in different shear failure modes. Zenodo 2020. https://doi.org/10.5281/zenodo.4059803.

[63] Lantsoght EOL. Shear in Reinforced Concrete Slabs under Concentrated Loads Close to Supports. Ph.D. Thesis , Faculty of Civil Engineering and Geosciences, Delft University of Technology, 2013.

[64] Cullington DW, Daly AF, Hill ME. Assessment of reinforced concrete bridges: Collapse tests on Thurloxton underpass. Bridg Manag 1996;Vol. 3:667–74.

[65] Lubell AS. Shear in Wide Reinforced Concrete Members. PhD dissertation. University of

Toronto, Canadá, 2006.

[66] Bui TT, Limam A, Nana W-S-A, Ferrier E, Bost M, Bui Q-B. Evaluation of one-way shear behaviour of reinforced concrete slabs: experimental and numerical analysis. Eur J Environ Civ Eng 2017:1–27. https://doi.org/10.1080/19648189.2017.1371646.

[67] Regan PE. Shear Resistance of Concrete Slabs at Concentrated Loads Close to Supports. Polytechnic of Central London, UK, 1982.

[68] Regan PE, Rezai-Jorabi H. Shear Resistance of One-Way Slabs Under Concentrated Loads. ACI Struct J 1988;85:150–7. https://doi.org/10.14359/2704.

[69] Vaz Rodrigues R, Muttoni A, Burdet O. Large Scale Tests on Bridge Slabs Cantilevers Subjected to Traffic Loads. Proc. 2nd Int. Congr. fib, Naples, Italy: 2006.

[70] Rombach GA, Latte S. Shear resistance of bridge decks without shear reinforcement. Proc. Int. fib Symp., Tailor Made Concrete Structures; 2008, p. 519–25. https://doi.org/doi:10.1201/9781439828410.ch86.

[71] Rombach G, Latte S. Querkrafttragfähigkeit Von Fahrbahnplatten Ohne Querkraftbewehrung. Beton- Und Stahlbetonbau 2009;104:642–56. https://doi.org/10.1002/best.200900029.

[72] Natário F, Fernández Ruiz M, Muttoni A. Experimental investigation on fatigue of concrete cantilever bridge deck slabs subjected to concentrated loads. Eng Struct 2015;89:191–203. https://doi.org/10.1016/J.ENGSTRUCT.2015.02.010.

[73] Henze L, Rombach GA. Versuche zur Querkrafttragfähigkeit von Stahlbetonplatten unter auflagernahen Einzellasten; Versuchsbericht (Experimental investigations on shear capacity of concrete slabs with concentrated loads close to the support). Hamburg: 2017. https://doi.org/10.15480/882.1443.

[74] Vida R, Halvonik J. Experimentálne overovanie šmykovej odolnosti mostovkových dosiek (Experimental verification of shear resistance of bridge deck slabs). Inžinierske Stavby/Inženýrské Stavby 2018:2–6.

[75] Reineck K-H, Bentz EC, Fitik B, Kuchma DA, Bayrak O. ACI-DAfStb Database of Shear Tests on Slender Reinforced Concrete Beams without Stirrups. ACI Struct J 2013;110:867–76. https://doi.org/10.14359/51685839.

[76] Collins MP, Bentz EC, Sherwood EG. Where is shear reinforcement required? Review of research results and design procedures. ACI Struct J 2008;105:590–600. https://doi.org/10.14359/19942.

[77] Muttoni A, Ruiz MF. Shear Strength of Members without Transverse Reinforcement as Function of Critical Shear Crack Width. ACI Struct J 2008;105:163–72. https://doi.org/10.14359/19731.

[78] Bentz EC, Vecchio FJ, Collins MP. Simplified modified compression field theory for calculating shear strength of reinforced concrete elements. ACI Struct J 2006;103:614–24. https://doi.org/10.14359/16438.

[79] Cavagnis F, Fernández Ruiz M, Muttoni A. Shear failures in reinforced concrete members without transverse reinforcement: An analysis of the critical shear crack development on the basis of test results. Eng Struct 2015;103:157–73. https://doi.org/10.1016/j.engstruct.2015.09.015.

[80] Yang Y. Shear Behaviour of Reinforced Concrete Members without Shear Reinforcement: A

New Look at an Old Problem. Delft University of Technology, 2014.

[81] Mihaylov BI, Bentz EC, Collins MP. Two-parameter kinematic theory for shear behavior of deep beams. ACI Struct J 2013;110:447–55. https://doi.org/10.14359/51685602.

[82] Lantsoght E, de Boer A, van der Veen C. Levels of approximation for the shear assessment of reinforced concrete slab bridges. Struct Concr 2017;18:143–52. https://doi.org/10.1002/suco.201600012.

[83] Bauer T, Müller M, Blase T. Strassenbrücken in Massivbauweise nach DIN-Fachbericht : Beispiele prüffähiger Standsicherheitsnachweise ; Stahlbeton- und Spannbetonüberbau nach DIN-Fachbericht 101 und 102 ; mit CD-ROM. Bauwerk; 2005.

[84] AASHTO. AASHTO LRFD Bridge Design Specifications. 8th Editio. Washington D.C.: American Association of State Highway and Transportation Officials (AASHTO); 2017.

[85] Rombach G, Henze L. Querkrafttragfähigkeit von Stahlbetonplatten ohne Querkraftbewehrung unter konzentrierten Einzellasten. Beton- Und Stahlbetonbau 2017;112:568–78. https://doi.org/10.1002/best.201700040.

[86] Muttoni A, Caldentey AP, Hegger J, Vill M, Shave JD, Menegotto M. PT-SC2-T1 D3BG - Background documents to prEN 1992-1-1:2018 2018.

[87] Reiβen K, Hegger J. Database of shear tests on RC slabs without shear reinforcement under concentrated loads – Assessment of design rules according to Eurocode 2. 16th Eur. Bridg. Conf., Edinburgh, Scotland: 2015.

[88] ACI Committee 318. Building Code Requirements for Structural Concrete (ACI 318-19) 2019:988.

[89] Vollum RL, Fang L. Shear enhancement near supports in RC beams. Mag Concr Res 2015;67:443–58. https://doi.org/10.1680/macr.14.00309.

[90] Sagaseta J, Vollum RL. Shear design of short-span beams. Mag Concr Res 2010;62:267–82. https://doi.org/10.1680/macr.2010.62.4.267.

[91] Krips M. Rißbreitenbeschränkung im Stahlbeton und Spannbeton (Crack width restriction in reinforced concrete and prestressed concrete). Berlin: Ernst & Sohn; 1985.

[92] Walraven JC. Aggregate Interlock: a Theoretical and Experimental Analysis. PhD. Thesis, Delft University of Technology, 1980.